CHEMISTRY
A EUROPEAN JOURNAL

DOI: 10.1002/chem.200800156

Fullerene C_{60}–Perylene-3,4:9,10-bis(dicarboximide) Light-Harvesting Dyads: Spacer-Length and Bay-Substituent Effects on Intramolecular Singlet and Triplet Energy Transfer

Jérôme Baffreau,[a] Stéphanie Leroy-Lhez,[a] Nguyên Vân Anh,[b] René M. Williams,*[b] and Piétrick Hudhomme*[a]

Abstract: Novel covalent fullerene C_{60}–perylene-3,4:9,10-bis(dicarboximide) (C_{60}–PDI) dyads (**1**–**4**) were synthesized and characterized. Their electrochemical and photophysical properties were investigated. Electrochemical studies show that the reduction potential of PDI can be tuned relative to C_{60} by molecular engineering through altering the substituents on the PDI bay region. It was demonstrated using steady-state and time-resolved spectroscopy that a quantitative, photoinduced energy transfer takes place from the PDI moiety, acting as a light-harvesting antenna, to the C_{60} unit, playing the role of energy acceptor. The bay-substitution (tetrachloro [**1** and **2**] or tetra-*tert*-butylphenoxy [**3** and **4**]) of the PDI antenna and the linkage length (C_2 [**1** and **3**] or C_5 [**2** and **4**]) to the C_{60} acceptor are important parameters in the kinetics of energy transfer. Femtosecond transient absorption spectroscopy indicates singlet–singlet energy-transfer times (from the PDI to the C_{60} unit) of 0.4 and 5 ps (**1**), 4.5 and 27 ps (**2**), 0.8 and 12 ps (**3**), and 7 and 50 ps (**4**), these values being ascribed to two different conformers for each C_{60}–PDI system. Subsequent triplet–triplet energy-transfer times (from the C_{60} unit to the PDI) are slower and in the order of 0.8 ns (**1**), 6.2 ns (**2**), 2.7 ns (**3**), and 9 ns (**4**). Nanosecond transient absorption spectroscopy of final PDI triplet states show a marked influence of the bay substitution (tetrachloro- or tetra-*tert*-butylphenoxy), and triplet-state lifetimes (10–20 μs) and the PDI triplet quantum yields (0.75–0.52) were estimated. The spectroscopy showed no substantial solvent effect upon comparing toluene (non-polar) to benzonitrile (polar), indicating that no electron transfer is occurring in these systems.

Keywords: dyes/pigments · energy transfer · fullerenes · light-harvesting · perylenediimide

Introduction

Photoinduced energy- and electron-transfer processes are crucial phenomena occurring in natural photosynthesis,[1] and the development of artificial photosynthetic systems is still of considerable interest for the elucidation of the mechanisms that convert sunlight into chemical energy.[2] Several strategies have been employed to mimic this natural photosynthetic system.[3] Among these, artificial light-harvesting antennas incorporated into molecular electron-donor–acceptor systems are prone to convert excitation energy into an electrochemical potential or chemical energy in the form of a long-lived charge-separation state. Fullerene C_{60} is now recognized to be a superior electron acceptor with regard to its inherent redox properties, low reorganization energy,[4] and highly symmetrical 3D structure,[5] and the porphyrins are the most frequently used electron donors in photosynthetic model systems.[6] In these molecular donor–acceptor dyads, intramolecular electronic interactions almost always

[a] Dr. J. Baffreau, Dr. S. Leroy-Lhez, Prof. P. Hudhomme
Université d'Angers, CNRS
Laboratoire de Chimie et Ingénierie Moléculaire d'Angers
CIMA UMR 6200, 2 Boulevard Lavoisier, 49045 Angers (France)
Fax: (+33) 241-735-405
E-mail: pietrick.hudhomme@univ-angers.fr

[b] N. Vân Anh, Dr. R. M. Williams
Molecular Photonics Group
Van't Hoff Institute for Molecular Sciences
Universiteit van Amsterdam
Nieuwe Achtergracht 129, 1018 WS Amsterdam (The Netherlands)
Fax: (+31) 205-256-456
E-mail: williams@science.uva.nl

Supporting information for this article is available on the WWW under http://www.chemeurj.org/ or from the author: Color versions of Figures 6–9, nano- and femtosecond transient absorption spectra of dyads **1**–**4**, ^{1}H NMR of compounds **1**, **3**, **12a**, **13a**, ^{13}C and HMBC, HMQC 2D NMR spectra of compounds **1** and **12a**.

dominate, generating (long- or short-lived) charge-separated states. Moreover, porphyrins have the advantage of being excellent light-harvesting antennas.[7] It was recently shown that such architectures can be tailored to construct molecular photonic devices as well as artificial photosynthetic systems. This kind of photoinduced electron transfer was recently extended to the production of photovoltaic cells that convert light into electric energy.[8] Attractive systems are now developed for the construction of organic solar cells, especially incorporating fullerene C_{60} in the photoactive layer.[9] In this area, the direct covalent bonding of various π donors to C_{60} has emerged as an active field of research.[10] However, for such application, back electron transfer and energy transfer from the donor to C_{60} are events to be minimized to increase the quantum yield and lifetime of charge separation.[11] Consequently, competition between energy- and electron-transfer in a functionalized electron-donor–fullerene dyad has to be carefully considered in designing new systems for photovoltaic applications. In many examples it was shown that efficient photoinduced electron transfer from a donor such as oligophenylenevinylene,[12] oligothiophene[13] or perylene[14] to fullerene C_{60} was the main pathway, whereas energy transfer could appear as a competitive process.[15]

Following the observation of the very fast photoinduced electron transfer occurring on the subpicosecond timescale from conducting polymers to C_{60},[16] a major breakthrough towards efficient organic photovoltaic devices was realized with the development of the bulk-heterojunction concept.[17] This approach consists of generating an interpenetrating network by blending the p-type electron-donating conjugated polymer and C_{60} or another fullerene derivative as n-type acceptor material.[18] In this field, intensive efforts on organic solar cells are still focused on interpenetrating networks using the soluble acceptor [60]PCBM.[19] However, the disadvantage of this fullerene derivative is its small molar absorption coefficient in the visible region. Consequently, one of the biggest challenges is now the access to materials that present the optimal absorption range, matching as well as possible the solar irradiation spectrum. This can be achieved with the development of p-type low band-gap polymers[20] that should increase the absorption in the visible and near-infrared (NIR) region of the solar spectrum. Another strategy concerns dendrimer-based light-harvesting structures that have attracted attention in the past decade.[21] The functionalization of C_{60} with oligomeric dendrons has given interesting light-harvesting systems in which peripheral chromophores are able to transfer the collected energy to the central core of the dendrimer.[22] Considering the n-type material incorporated in the blend, the improvement of the light absorption of fullerene derivatives and its relationship with the efficiency of photovoltaic cells was demonstrated with the replacement of the C_{60} derivative by the C_{70} analogue.[23]

We are interested in the concept of linking a dye molecule to fullerene C_{60} as a potential system presenting efficient light-harvesting properties. The idea behind this is that the dye could act as an antenna by absorbing sunlight, thereby inducing an intramolecular energy transfer towards the fullerene. Perylene-3,4:9,10-bis(dicarboximide) (PDI) dyes were chosen as potential antennas because of their high chemical stability, high photoluminescence quantum yield, and the possibility for tuning the absorption range by variation of the substitution pattern on the perylene core. During the last few years, PDI derivatives have been developed as one of the most useful classes of chromophores.[24] One of the most active areas of research involving PDI systems is related to their utilization in photoinduced electron- and/or energy-transfer processes. In this regard, electroactive units such as fluorenone and anthraquinone,[25] tetrathiafulvalene,[26] pyrene,[27] oligothiophene,[28] zinc phthalocyanine,[29] 3,4-ethylenedioxythiophene,[30] zinc porphyrin,[31] hexaazatriphenylenes,[32] anthracene dendrimers,[33] perylenemonoimide,[34] tetraboron-dipyrrin,[35] and poly(fluorene-*alt*-phenylene)[36] were connected to the PDI dye to reach molecular ensembles in which an electron- and/or energy-transfer event occurs. In the search for such electronic interaction involving PDI, supramolecular architectures were also recently described involving an oligo(*p*-phenylenevinylene),[37] a

Abstract in French: *De nouveaux assemblages covalents fullerène C_{60}–pérylène-3,4:9,10-bis(dicarboximide) (C_{60}–PDI) (**1**–**4**) ont été synthétisés et caractérisés. Les propriétés électrochimiques et photophysiques ont également été établies. Par ingénierie moléculaire et en jouant sur la nature des substituants présents sur le noyau PDI, le premier potentiel de réduction du PDI peut être modulé par rapport à celui de C_{60}. Les études spectroscopiques à l'état stationnaire et en temps résolu ont permis de mettre en évidence un transfert d'énergie photoinduit quantitatif intervenant de la partie PDI jouant le rôle d'antenne vers l'accepteur C_{60}. Par ailleurs, la nature des substituants (tétrachloro pour **1** et **2**, ou tétra-*tert*-butylphénoxy pour **3** et **4**) sur l'unité PDI et la longueur de l'espaceur (C_2 pour **1** et **3** ou C_5 pour **2** et **4**) entre le PDI et le fullerène C_{60} sont des paramètres importants sur les cinétiques de transfert d'énergie. La spectroscopie d'absorption transitoire femtoseconde indique des temps de transfert d'énergie singulet–singulet du PDI vers le C_{60} de 0.4 et 5 ps (pour **1**), 4.5 et 27 ps (pour **2**), 0.8 et 12 ps (pour **3**), 7 et 50 ps (pour **4**), attribués à la présence de deux conformations privilégiées pour chaque système C_{60}–PDI. Par ailleurs, les temps de transfert d'énergie triplet–triplet de C_{60} vers le PDI sont plus lents et de l'ordre de 0.8 ns (pour **1**), 6.2 ns (pour **2**), 2.7 ns (pour **3**) et 9 ns (pour **4**). La spectroscopie d'absorption transitoire nanoseconde montre que l'état triplet final du PDI dépend de la nature de la substitution. Des durées de vie de l'état triplet de 10–20 μs et des rendements quantiques de 0.75–0.52 ont été déterminés. Aucun effet significatif en fonction de la nature non-polaire (toluène) ou polaire (benzonitrile) du solvant n'a été mis en évidence, indiquant qu'aucun transfert d'électron ne semble intervenir au sein de ces systèmes.*

bis(ruthenium phthalocyanine) moiety,[38] or zeolite crystals.[39]

In the last three years, and in parallel to our first investigation,[40] new electroactive PDI-based systems involving the attractive fullerene C_{60} electron acceptor were considered and the synthesis of many C_{60}–PDI dyad or triad systems have now been reported.[41] Nevertheless, the spectral and kinetic characterization of the photoinduced processes that are inherent to the combination of these electroactive units have received little attention. It was only recently shown that an efficient photoinduced electron transfer occurs in the C_{60}–PDI dyad in which electron-donating pyrrolidino groups are introduced on the bay region of the PDI moiety.[41g,h] The consequence of such substitution is the corresponding low oxidation potential of the PDI moiety, thus facilitating the electron transfer from PDI to C_{60}.

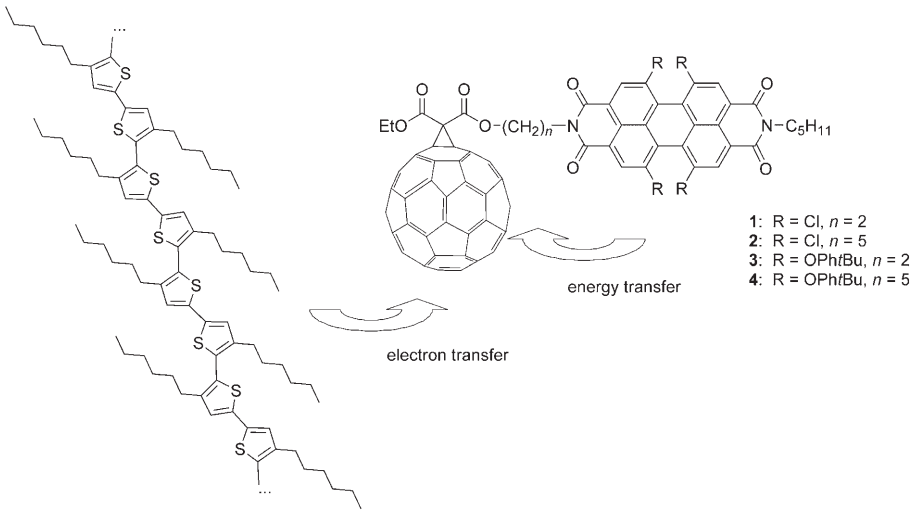

Scheme 1. Representation of the photoactive layer of an organic solar cell incorporating the p-type P3HT polymer donor and the C_{60}–PDI dyad.

In this paper we describe the synthesis as well as the electrochemical and photophysical properties of C_{60}–PDI dyads **1**–**4** in the search for an efficient energy transfer from PDI to C_{60}. In designing these systems it was assumed that the distance between PDI and C_{60} moieties and their mutual orientation could be crucial parameters for the rate of energy transfer and could play an important role in the electronic interaction between both partners. Another objective was to demonstrate that the nature of the substituents on the PDI bay region strongly influence the electronic properties of these dyads for their further utilization in photovoltaic devices. In designing these solar cells it is considered that inside the photoactive layer the following events occur: 1) self-assembly into an interpenetrating nanoscopic network, 2) an energy transfer from PDI towards fullerene C_{60} with the dye acting exclusively as a light-harvesting antenna, and 3) a selective electron transfer between the p-type polymer donor such as poly3-hexylthiophene (P3HT) to the C_{60} unit (Scheme 1). We report here on the second point, that is, energy-transfer phenomena occurring from the PDI unit towards fullerene C_{60} and on the influence of the spacer length and bay substitution of the PDI on the kinetics and spectral features.

Results and Discussion

Synthesis: The strategy employed for the preparation of C_{60}–PDI dyads **1**–**4** is based upon the cyclopropanation reaction, which has proven to be very efficient for the functionalization of C_{60}. Consequently, initial efforts were focused on the synthesis of unsymmetrical PDI precursors. Methods to reach unsymmetrical 3,4:9,10-perylenetetracarboxylic monoanhydride monoimide derivatives non-substituted at the bay region have been reported previously.[42] Application of these strategies on 1,6,7,12-tetrachloro-3,4:9,10-perylene tetracarboxylic dianhydride **5** as starting material proved to be fastidious. As an alternative method, we achieved the direct condensation of PDI **5** with pentan-1-amine and 2-aminoethanol or 5-aminopentan-1-ol in stoichiometric ratio (Scheme 2). Unsymmetrical (**6a** or **6b**) and symmetrical (**7** and **8a** or **8b**) PDI compounds were efficiently separated by silica-gel column chromatography thanks to the difference in their respective polarity. This method constitutes an efficient synthesis of unsymmetrical PDI **6a** or **6b** bearing the alcohol functionality after its separation from *N*,*N*′-dipentylPDI derivative **7** and symmetrical PDI dialcohols **8a** or **8b**.

The introduction of *tert*-butylphenoxy groups at the bay region to achieve *tert*-butylphenoxyPDI **9a** and **9b** was carried out using a nucleophilic substitution of chlorine atoms with 4-*tert*-butylphenol in the presence of potassium carbonate according to a well-known strategy.[43] Another route was attempted to synthesize compound **9a** starting from *N*,*N*′-dipentylPDI derivative **7** previously obtained as a by-product. The latter was firstly transformed into the corresponding *tert*-butylphenoxyPDI **10** in 69% yield following a similar nucleophilic-substitution reaction. Subsequent treatment with potassium hydroxide in *tert*-butyl alcohol[42c,44] gave the corresponding dianhydride **11** in 93% yield. Unsymmetrical PDI **9a** was obtained in 34% yield by condensation of pentan-1-amine and 2-aminoethanol in stoichiometric ratio followed by separation from both symmetrical PDI derivatives (Scheme 3).

Subsequent transformation of the alcohol into the malonate functionality was performed using ethyl malonyl chloride in the presence of pyridine and corresponding derivatives **12** and **13** were isolated in satisfactory yields (Scheme 4). Reaction of cyclopropanation was carried out

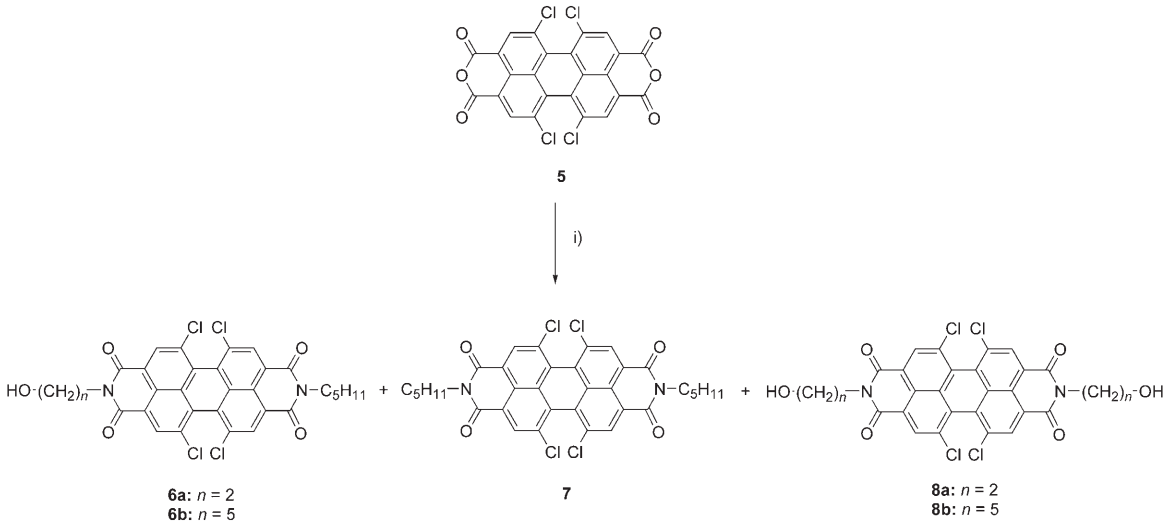

Scheme 2. i) $C_5H_{11}NH_2/HO(CH_2)_nNH_2$ 1:1, toluene, reflux, then column chromatography (**6a**: 28%, **6b**: 17%).

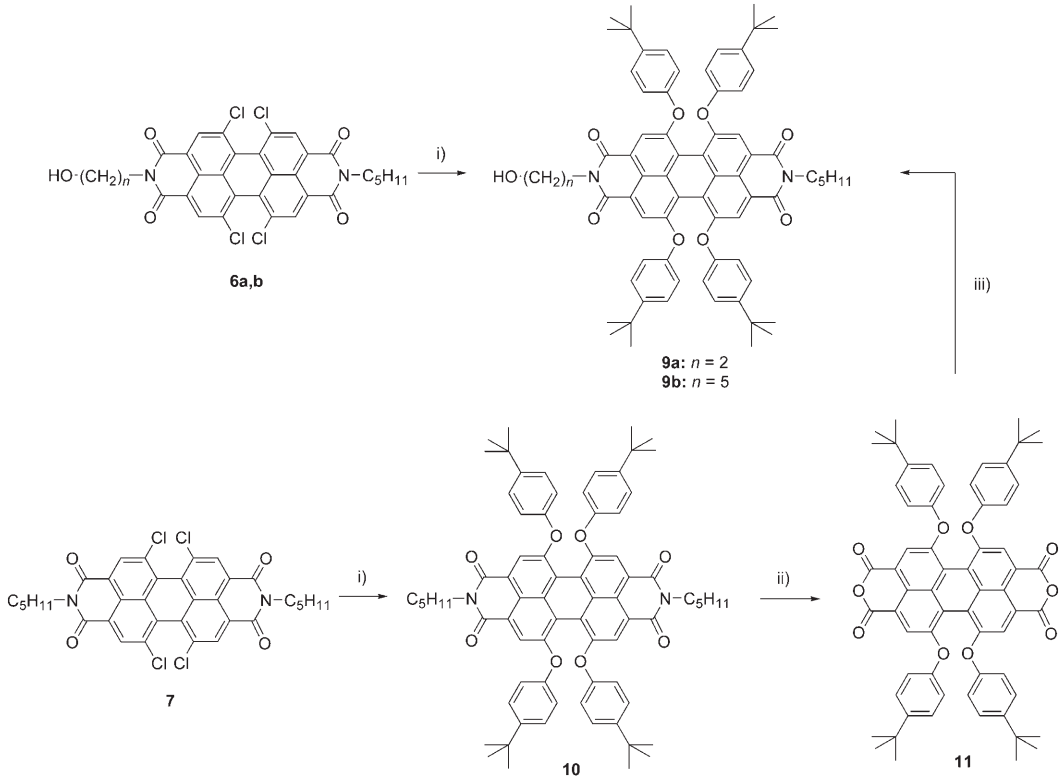

Scheme 3. i) *p-tert*-Butylphenol, K_2CO_3, *N*-methylpyrrolidone, 130°C, (**9a**: 60%, **9b**: 58%; **10**: 69%); ii) KOH, *t*BuOH, reflux, then 1N HCl, 93%; iii) $C_5H_{11}NH_2/HO(CH_2)_2NH_2$ 1:1, toluene, reflux, then column chromatography, 34%.

by reaction with C_{60} in the presence of iodine and 1,8-diazabicyclo[5.4.0]undec-7-ene (DBU).[45] Methano[60]fullerene dyads **1**–**4** were purified by silica-gel column chromatography.

With the aim of simplifying the synthetic scheme of dyads **3** and **4**, we considered the straightforward post-functionalization of dyads **1** and **2**, respectively. Attempts to replace chlorine atoms of dyad **1** by *tert*-butylphenoxy groups to yield dyad **3** according to the reaction as described above were unsuccessful. Using such experimental conditions on dyad **1**, the nucleophilic substitution of chlorine atoms by *tert*-butylphenoxy groups was accompanied by the concomitant cleavage of the malonate functionality and the unique alcohol **9a** was isolated in 66% yield.

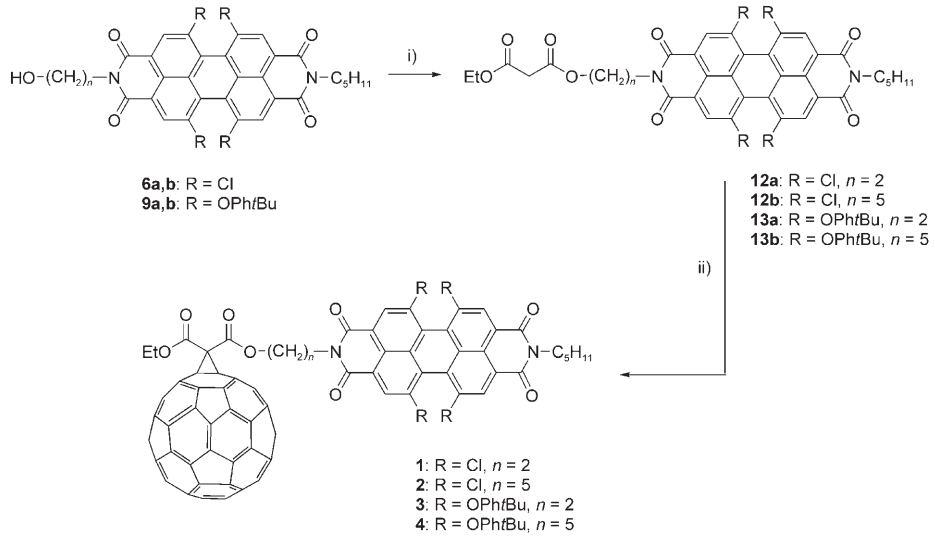

Scheme 4. i) $ClCOCH_2CO_2Et$, pyridine, CH_2Cl_2, (**12a**: 93%, **12b**: 94%, **13a**: 91%, **13b**: 88%); ii) C_{60}, DBU, I_2, toluene, (**1**: 53%, **2**: 42%, **3**: 47%, **4**: 51%).

^{1}H NMR spectroscopy: To evaluate the extent of the interaction between C_{60} and PDI units in solution, ^{1}H NMR spectra of dyads **1** and **3** were compared with those of their malonate precursors **12a** and **13a**, respectively. ^{1}H NMR spectra of compounds **12a** and **13a** ($CDCl_3$, 293 K) show that the four protons of the -NCH_2-CH_2O- linkage fortuitously present a single signal at 4.55 ppm for PDI **12a** and at 4.45 ppm for PDI **13a**. This observation was confirmed by HMBC and HMQC 2D NMR correlated spectra carried out on compound **12a** (Supporting Information). It is worth noting that the case of dyad **1** appears very different from its precursor **12a**. In the ^{1}H NMR spectrum of dyad **1** recorded in $CDCl_3$ at 293 K, the ethylene linkage appears as a four-proton spin system, demonstrating the non-equivalence of the four protons (Figure 1a). At this stage it is important to note that the C_{60} unit in dyad **1** is also responsible for an important deshielding effect on these four -NCH_2-CH_2O- protons (up to $\Delta\delta = 0.54$ ppm) compared to **12a**, as well as for the -CH_2- protons of the ethyl ester functionality ($\Delta\delta = 0.44$ ppm). In agreement with HMQC correlation technique, both signals centered at 5.09 and 4.78 ppm were assigned to the -OCH_2 group (noted H_A and $H_{A'}$, respectively), and signals at 4.92 and 4.62 ppm to the -NCH_2 group (noted H_B and $H_{B'}$, respectively) (Figure 1a). The corresponding coupling constants are of $^2J = 14$ Hz (geminal protons), $^3J = 3.5$ and 8.5 Hz. According to the Karplus equation[46] and its application in determining the conformations of ethane derivatives,[47] dihedral torsion angles of approximately 45° and 165° were estimated for dyad **1** using these ^3J coupling constants. Consequently, two preferential conformations of the -NCH_2-CH_2O- linkage can be considered from these parameters (Figure 1b), as was also predicted by theoretical calculations.[48] Variable-temperature NMR experiments were conducted at 313 K and 343 K, but no evolution in the different coupling constants was observed (Figure 1c). Interestingly, a significant linear dependence of the chemical shift on temperature was noted for each proton, with a shielding effect for A and B protons, and on the contrary a deshielding effect for A′ and B′ protons (Figure 1d).

The ^{1}H NMR spectrum of dyad **3** recorded in $CDCl_3$ at 293 K presents a similar behavior, but the signals corresponding to the -NCH_2-CH_2O- linkage appear broader than in the case of dyad **1**. We assign this difference to spin relaxation resulting from the strong steric hindrance between the fullerene and the *tert*-butylphenoxy groups on the bay region of the PDI. Here again, the -NCH_2-CH_2O- linkage appears as a series of four signals (4.90, 4.82, 4.72, and 4.64 ppm) that are deshielded relative to precursor **13a** (up to $\Delta\delta = 0.45$ ppm). A variable-temperature NMR study showed a clear narrowing of all the peaks with a coalescence phenomenon arising at 313 K for both -NCH_2 and -OCH_2 groups (Figure 1e).

These ^{1}H NMR studies clearly demonstrate the presence of a restricted rotation inducing conformational effects around the -NCH_2CH_2O- linkage in dyads **1** and **3**. This phenomenon as well as the temperature-dependent dynamic effect observed for dyad **3** can be unambiguously attributed to the presence of C_{60}.[49]

As a high purity of the compounds is crucial for further photophysical studies, an efficient way to purify dyads **1**–**4** and reference compounds was needed. For this purpose, analytical and semi-preparative HPLC were carried out on a silica column using toluene/CH_2Cl_2 3:1 for dyad **1**–**4** and tetrachloro-substituted PDI **7**. For tetraphenoxy-substituted PDI **10** and 1,1-di(ethoxycarbonyl)-[6,6]-methanofullerene **14**, the latter being prepared starting from α-bromoethyl malonate as reported in the literature (Scheme 5),[50] toluene was used as the eluent for analytical and semipreparative HPLC. The purity of dyads **1**–**4** was estimated to be superior to 99.9%.

Electrochemical properties: Cyclic voltammetry was used to electrochemically characterize dyads **1**–**4** (Table 1). Compounds **7**, **10**, and **14** were used as references allowing the determination of the nature of reduced species. Dyad **1** showed three reversible reduction waves and the first one-electron process at $E^0_{red1} = -0.84$ V (vs Fc^+/Fc) was assigned to the formation of the anion radical of the PDI moiety (C_{60}–$PDI^{\bullet-}$). The following two one-electron reduction process at $E^0_{red2} = -1.08$ V corresponding to the generation of the $C_{60}^{\bullet-}$–PDI^{2-} species suggested that the first reduction wave of fullerene and the second reduction wave of PDI were overlapping. The third one-electron wave appearing at

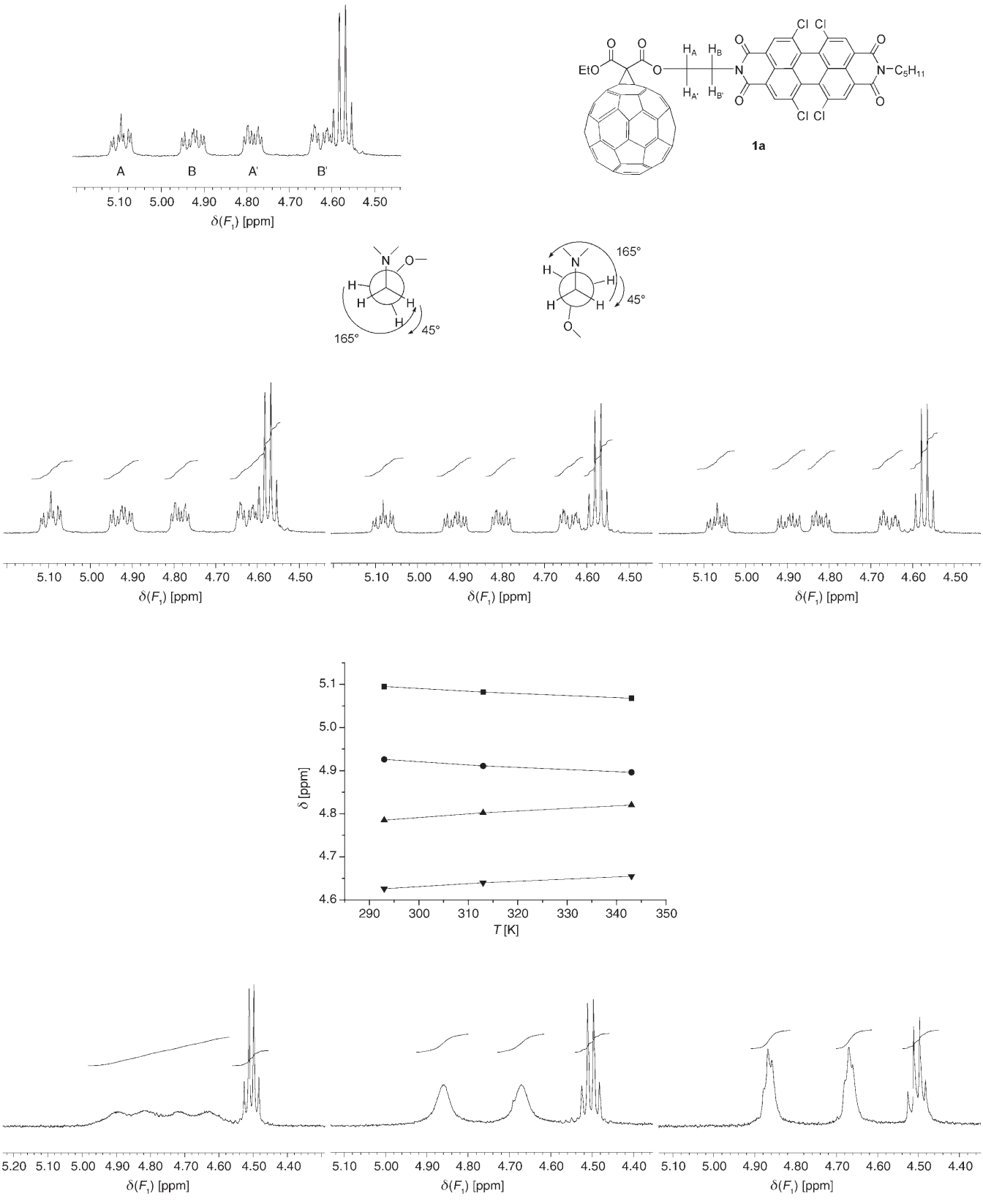

Figure 1. a) ^{1}H NMR spectra of the -NCH_2-CH_2O- linkage in dyad **1** at 293 K; b) folded (left) and extended (right) conformations in dyad **1** derived from the coupling constants using the Karplus equation; c) ^{1}H NMR spectra of dyad **1** at 293 K (left), 313 K (center), and 343 K (right); d) linear temperature dependence of protons A (■), B (●), A′ (▲), and B′ (▼) chemical shifts in dyad **1**; e) ^{1}H NMR spectra of dyad **3** at 293 K (left), 313 K (center), and 343 K (right).

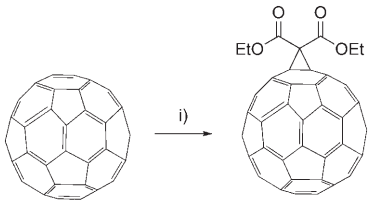

14

Scheme 5. i) EtO_2C-CHBr-CO_2Et, NaH, toluene, 57%.

Table 1. Redox-potential values (vs Fc^+/Fc) of dyads **1**–**4** and reference compounds **7**, **10**, and **14** recorded in a CH_2Cl_2 solution using Bu_4NPF_6 0.1 M as the supporting electrolyte, Ag wire as the reference, platinum wires as counter and working electrodes. Scan rate: 100 mV s^{-1}.

Compound	E^0_{red4} [V]	E^0_{red3} [V]	E^0_{red2} [V]	E^0_{red1} [V]	E^0_{ox1} [V]	E^0_{ox2} [V]
1	–	−1.47	−1.08[a]	−0.84	+1.24[b]	
2	−1.87[b]	−1.45	−1.07[a]	−0.86	–	
3	−1.46	−1.35	−1.24	−1.10	+0.83	+1.23[b]
4	−1.44	−1.37	−1.23	−1.09	+0.82	–
7			−1.06	−0.87	–	–
10			−1.37	−1.21	+0.80	+1.14
14			−1.47	−1.08	+1.22[b]	–

[a] Two one-electron process. [b] Irreversible process.

$E^0_{red3} = -1.47$ V resulted from the formation of C_{60}^{2-}–PDI^{2-} species. One irreversible oxidation process was observed at $E^0_{ox1} = +1.24$ V.

Cyclic voltammogram of dyad **3** showed four reversible one-electron reduction waves. The first process arising at $E^0_{red1} = -1.10$ V (vs Fc^+/Fc) was assigned to the formation of the anion radical of the C_{60} moiety ($C_{60}^{-\bullet}$–PDI). This was followed by both one-electron reduction processes of the PDI moiety leading successively to $C_{60}^{-\bullet}$–$PDI^{-\bullet}$ ($E^0_{red2} = -1.24$ V) then $C_{60}^{-\bullet}$–PDI^{2-} species ($E^0_{red3} = -1.35$ V). The fourth one-electron reduction wave was corresponding to the generation of the C_{60}^{2-}–PDI^{2-} species at $E^0_{red4} = -1.46$ V. A first reversible one-electron oxidation process arising at $E^0_{ox1} = +0.83$ V was followed by an irreversible wave appearing at $E^0_{ox2} = +1.23$ V.

Considering the cyclic voltammogram of dyads **2** and **4**, it should be noted that the influence of the length of the alkyl chain on the imide position is not characteristic. The reason is that the imide nitrogen atoms correspond to nodes in the LUMO of PDI derivatives, thus indicating that substituents at those positions do not really influence the corresponding energy levels.[51]

It was reported in the case of C_{60}–PDI dyads with PDI bearing only hydrogen atoms at the bay region[41d] that the first reduction potential corresponds to a reversible two one-electron process leading directly to the $C_{60}^{-\bullet}$–$PDI^{-\bullet}$ species. In the case of dyads **1** and **2** with the PDI substituted by four chlorine atoms at the bay region, the first reduction occurs on the PDI moiety. The enhancement of the electron affinity is explained by the electron-withdrawing inductive effect of the chlorine atoms stabilizing the anion radical $PDI^{-\bullet}$, this minimizing their possible electron-donating mesomeric effect. For dyads **3** and **4** with the PDI bearing *tert*-butylphenoxy groups at the bay region, the C_{60} moiety appears to be the favored electron acceptor. In the latter case, the electron-donating mesomeric effect of phenoxy groups appeared predominant with less consideration for their possible electron-withdrawing inductive effect. This demonstrates that electronic properties of C_{60}–PDI dyads can be perfectly tuned thanks to a well-defined substitution of the PDI bay region.

Electronic absorption: Electronic absorption spectra of dyads **1**–**4** and reference compounds **7**, **10**, **14** were recorded in toluene and dichloromethane at room temperature (Figure 2 and Table 2). No significant solvent effect was observed, but further insight into solvatochromism was prevented by the lack of solubility of the dyads. All compounds containing the PDI unit exhibit the three typical absorption peaks at approximately 430, 485, and 520 nm for **1**, **2**, and **7** or 450, 540, and 580 nm for **3**, **4**, and **10**. The values reported for a PDI derivative bearing hydrogen atoms at the bay region are intermediate (434, 460, 491, and 528 nm).[52,53] In agreement with information issued from electrochemical analyses, the hypsochromic effect observed for **1**, **2**, and **7** could be ascribed to the bay-substitution pattern of the PDI moiety and, more precisely, of the electron-withdrawing inductive effect of chlorine atoms. On the other hand, the bathochromic effect for **3**, **4**, and **10** could be related to the electron-donating mesomeric effect of phenoxy groups. It appears that electronic effects are predominant.[24] The expected hypsochromic effect due to the decrease of conjugation because of the torsion induced by the bay substitution is negligible. According to literature,[52,53] these bands could be attributed to the transitions 3–0, 1–0, 0–0, with a weak transition 2–0 that could be only

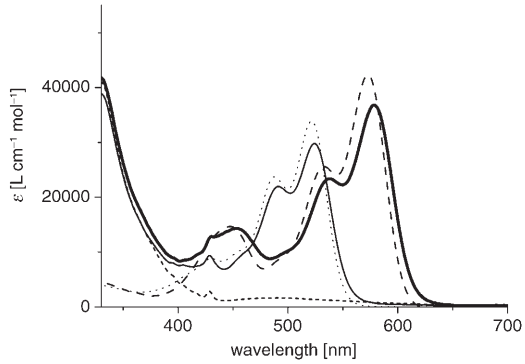

Figure 2. Absorption spectra of dyads **1** (——) and **3** (——) and reference compounds **7** (•••••), **10** (-----), and **14** (– – –) in toluene at 298 K ($c < 10^{-6}$ M).

Table 2. Electronic absorption data for dyads **1**–**4** and reference compounds **7**, **10**, **14**.[a]

	Toluene		Dichloromethane	
	λ_{max} [nm]	ε_{max} [$M^{-1}cm^{-1}$]	λ_{max} [nm]	ε_{max} [$M^{-1}cm^{-1}$]
1	524	29800	522	32800
2	522	31350	520	32800
3	579	36800	586	38500
4	576	37300	582	38500
7	522	33900	518	40300
10	575	42000	582	42700
14	689 (490, 428)	250 (1700, 3000)	693 (496, 431)	105 (1400, 2500)

[a] Other absorption bands of compound **14** and their respective molar absorption coefficients.

barely distinguished around 460 nm for **7** and 500 nm for **10**. The extinction coefficient values found are in agreement with those reported in literature and are within the range 30000–40000 cm^{-1} for these compounds.[26b,54] The strong absorption band at 330 nm observed for **1**–**4** and **14** was ascribed to fullerene C_{60} absorption. The sharp peak at 430 nm observed for **14** is characteristic of [6,6]-methanofullerene derivatives, as well as the peak at approximately 690 nm that corresponds to the $S_1 \leftarrow S_0$ transition.[55] Rather similar spectral features are also observed for pyrrolidine C_{60} derivatives[55b] and for C_{60} Diels–Alder adducts.[55c] Moreover, the UV-visible absorption spectra of dyads **1**–**4** match the profile obtained by superposition of the spectra of corresponding reference compounds **7** or **10** and **14**. Independently of the bay-substitution pattern or spacer length between PDI and C_{60} moieties, this characterizes the absence of significant interaction in the ground state between these two partners.

Fluorescence emission: Fluorescence emission spectra of reference compounds **7**, **10**, and **14** were recorded in toluene and dichloromethane and were found to be independent of the excitation wavelength (Figure 3A and Table 3).

Fluorescence excitation spectra matched the absorption profile over the entire wavelength range. As expected, PDI-based compounds **7** and **10** are strongly emissive in the visible range with fluorescence quantum yields being close to unity at room temperature. On the other hand, compound **14** presented a typical weak emission centered at 697 nm with a fluorescence quantum yield of approximately 5×10^{-4} at room temperature, characteristic of [6,6]-methanofullerene derivatives.[55–57] All the fluorescence emission spectra of dyads **1**–**4** are composed of two bands, one characteristic of the PDI moiety in the 500–650 nm range, the second corresponding to the methanofullerene in the 670–750 nm region (Figure 3B and Table 3). The very weak importance of C_{60} emission in dyad **2** relative to dyad **1** should be noticed. The spacer length between PDI and C_{60} seems to have an influence on the relative intensity of these two bands. For dyads **3** and **4** bearing *tert*-butylphenoxy groups at the bay area, a bathochromic shift of the emission maxima was noticed in agreement with the absorption spectrum. The consequence is an overlapping of emissions centered on the PDI and C_{60} moieties.

The Stokes' shift values in both toluene and dichloromethane are in the 700–900 cm^{-1} range, except for **14** for which the Stokes' shift value is smaller (Table 3), all these values being coherent with a weak geometrical reorganization of the considered fluorophore at the excited state (PDI for **1**–**4**, **7**, **10** and C_{60} for **14**). Moreover,

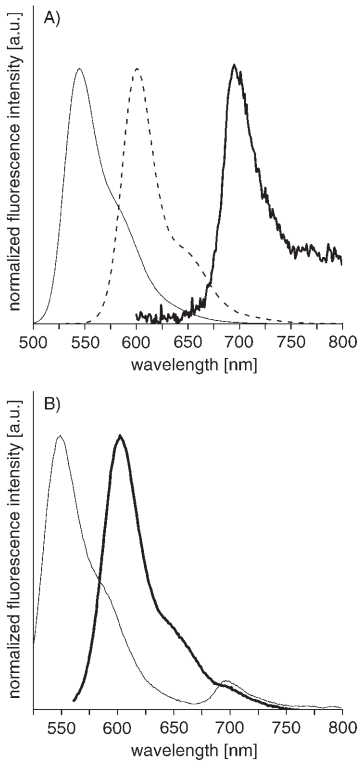

Figure 3. Emission spectra of A) reference compounds **7** (——, λ_{exc} = 485 nm), **10** (-----, λ_{exc} = 550 nm), and **14** (——, λ_{exc} = 450 nm) and B) dyads **1** (——, λ_{exc} = 520 nm) and **3** (——, λ_{exc} = 550 nm) in toluene at 298 K ($c < 10^{-6}$ M).

Table 3. Photophysical properties (emission) of dyads **1**–**4** and reference compounds **7**, **10**, **14** at 298 K.

	Toluene					Dichloromethane		
	λ_{max} [nm]	$\Delta\tilde{\nu}$ [cm^{-1}]	Φ_f	τ [ps]	$k_{en} \times 10^{10}$ [s^{-1}]	λ_{max} [nm]	$\Delta\tilde{\nu}$ [cm^{-1}]	Φ_f
1	549 (696)	909	3.3×10^{-3}	9	11.1	545 (694)	808	2.3×10^{-3}
2	548 (696)	923	3.8×10^{-3}	30	3.3	545 (696)	882	3.1×10^{-3}
3	602 (698)	808	3.4×10^{-3}	25	3.9	609 (694)	808	2.5×10^{-3}
4	600 (697)	694	4.6×10^{-3}	54	1.8	608 (694)	923	3.2×10^{-3}
7	548	923	1	5580	–	544	923	1
10	601	923	1	5950	–	607	882	1
14	697	167	5.0×10^{-4}	1500[a]	–	696	62	5.0×10^{-4}

[a] In good agreement with ref. [55a].

there is a dramatic quenching of the PDI fluorescence emission for all the dyads. At room temperature, the fluorescence quantum yields are in the range $2–3\times10^{-3}$, this being also dependent on the spacer length. Considering identical bay substitution, the shorter the alkyl chain between PDI and C_{60} units, the stronger the fluorescence quenching.

This strong quenching (up to 99.8%, depending on the dyad) should result from an intramolecular interaction between PDI and C_{60} in the excited state as the quantum yield of neither **7** nor **10** was affected by the addition of up to ten equimolecular amounts of **14** in solution. To get further insights into the nature of this new process, the fluorescence emission spectrum of **1** was recorded by selectively exciting the PDI unit in the dyad (Figure 3B). The C_{60} emission features are still observed, evidencing a singlet–singlet energy transfer between PDI and C_{60}. This process is in agreement with the energy levels of both PDI and C_{60} units, 2.32 eV for **7** and 1.79 eV for **14** in toluene. This was confirmed by the excitation spectrum recorded at 695 nm in dichloromethane. Indeed, the characteristic absorption bands of PDI are still present in this spectrum (Figure 4).

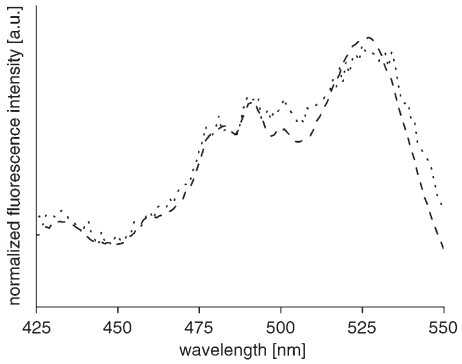

Figure 4. Excitation spectra of dyad **1** at $\lambda_{obs}=570$ nm (•••••) and at $\lambda_{obs}=695$ nm (-----) in dichloromethane at 298 K ($c<10^{-6}$ M).

Similar experiments could not be conducted for dyads **3** or **4** as fluorescence emissions of PDI and C_{60} are overlapping. Nevertheless, by subtracting the contribution of PDI from the emission spectrum of **3** or **4**, the fullerene emission is still observed, even when the PDI is selectively excited at wavelengths above 550 nm.[40] This result associated with the strong fluorescence quenching of PDI emission corroborates the hypothesis of an energy transfer from PDI to C_{60} for these dyads. Energy levels are still in agreement as the first excited state of **10** is lying at 2.11 eV, that is, 0.32 eV above the first excited state of compound **14** in toluene (Table 4).

Altogether these results underline the efficiency of this process as a function of bay-area substitution and spacer length. Indeed, the quenching of fluorescence appears higher for chlorine-substituted dyad **1** than with *tert*-butylphenoxy-substituted dyad **3** (Table 3). This phenomenon is confirmed by the emission spectra of dyads **1**–**4** recorded in rigid solvent glass (methylcyclohexane/toluene 7:3) at low temperature (77 K) (Figure 5A and B). A slight bathochromic shift with decreasing temperature for fluorescence emission of dyads **1** and **2** was noticed ($\Delta\lambda_{max}=11$ nm between 77 K and room temperature). These spectra showed well-structured vibronic bands in agreement with the lack of solvent relaxation in rigid medium. Consequently, at 77 K a better comparison of the intensity ratio between the PDI emission band (550 nm for dyads **1** and **2** and 600 nm for dyads **3** and **4**) and the C_{60} emission band (ca. 700 nm) could be performed. Considering the same bay substitution and PDI fluorescence-emission intensity being normalized, it was clearly displayed from these spectra that C_{60}-centered emission is more important for dyads presenting the shortest spacer, thus confirming the real influence of the spacer length on the efficiency of energy transfer between PDI and C_{60}. Furthermore, no phosphorescence emission was detected under these experimental conditions.

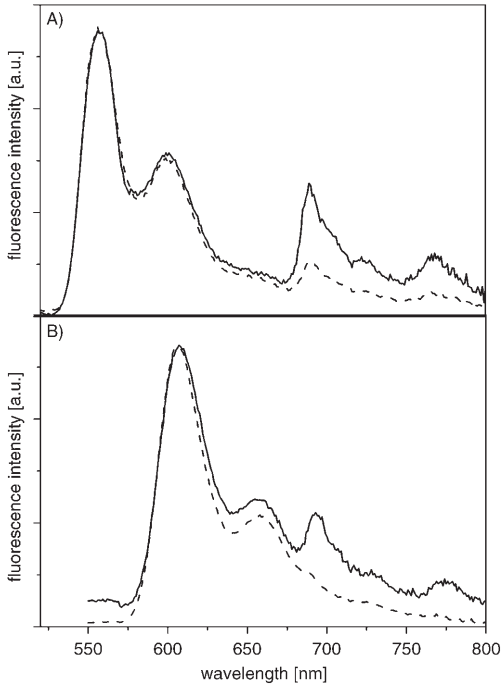

Figure 5. Normalized fluorescence emission spectra at 77 K in methylcyclohexane/toluene 7:3 matrix: A) for dyads **1** (——) and **2** (-----, $\lambda_{exc}=490$ nm); B) for dyads **3** (——) and **4** (-----, $\lambda_{exc}=450$ nm).

Table 4. Energy level of the charge-separated state for dyads **1**–**4** and parameters used for the calculation.

Dyad	E_{ox}[a] [eV]	E_{red}[a] [eV]	E^{0-0} [eV]	ΔG [eV]	Energy level [eV]		
					E_{PDI}	E_{CS}	E_{C60}
1	+1.24	−0.84	2.32	−0.24	2.33	2.09	1.79
2	+1.24	−0.84	2.32	−0.24	2.33	2.09	1.79
3	+0.83	−1.10	2.11	−0.18	2.11	1.93	1.79
4	+0.83	−1.10	2.11	−0.18	2.11	1.93	1.79

[a] vs Fc^+/Fc in CH_2Cl_2.

The intramolecular energy transfer from PDI to C_{60} could be discussed in terms of Coulombic interactions (Förster)[58] or exchange interactions (Dexter).[59]

In order to know if this energy transfer could be due to Coulombic interaction, Förster radii R_0 were calculated for each dyad (Table 5), according to Equation (1):[58]

$$R_0 = 0.2108[\kappa^2 \phi_D^0 n^{-4} \int_0^\infty I_D(\lambda)\varepsilon_A(\lambda)\lambda^4 d\lambda]^{1/6} \quad (1)$$

where κ is the orientation factor, ϕ_D^0 is the emission quantum yield of the reference donor chromophore, $I_D(\lambda)$ is the corrected fluorescence intensity of the donor with the total intensity normalized to unity and n is the refractive index of the solvent. For dyads **1**–**4**, ϕ_D^0 is equal to one and κ^2 to $^2/_3$ because of the random orientation of the dipole between molecules. All the values obtained for R_0 in both toluene and dichloromethane are superior to the distance calculated by molecular optimization between PDI and C_{60} for each dyad.[48] According to this result, the nature of the energy transfer to dyads **1**–**4** should be of Förster type. Using these R_0 values and the experimental rates, center-to-center distances could be estimated (Supporting Information).

Table 5. Calculated Förster radii R_0 [Å] for dyads **1**–**4**.

	Toluene	Dichloromethane
1	32.3	31.5
2	32.3	31.5
3	28.1	30.0
4	28.1	30.0

To study the possibility of a competitive reductive (for dyads **1** and **2**) or oxidative (for dyads **3** and **4**) electron-transfer process, the "Gibbs energy of photoinduced electron transfer" was estimated for each dyad.[60] For all the dyads, the corresponding charge-separated state lies at an intermediate energy level between the fullerene and PDI singlet-excited states (Table 4). If the Coulomb and solvent-correction terms are taken into account, the energy level will be lowered, making it energetically more accessible in dichloromethane and benzonitrile. In toluene, however, charge separation would be an endergonic process (using "average" center-to-center distances, listed in Supporting Information, and average ionic radii of 4 Å). Apparently the excited-state processes in polar solvents are governed by kinetic factors: charge separation is energetically possible, but it is not observed (see below).

Time-resolved spectroscopy: To get more information on the effects of the bay substitution and the spacer length on the interaction between the fullerene unit and the PDI chromophore, various types of time-resolved spectroscopy were applied. The photophysical properties of the systems (**1**–**4**) containing fullerene C_{60} covalently linked to the perylenediimide as well as those of the reference compounds **7**, **10**, and **14** in toluene were investigated. Benzonitrile as a solvent was also used to check the presence of electron transfer in polar solvents in some femto- and nanosecond transient absorption experiments.

Single photon counting (SPC): SPC was used to determine the emission decays of the dyads **1**–**4** and the reference systems **7**, **10**, and **14** in toluene. The decay curves recorded for dyads **1** and **2** (at 550 nm) and dyads **3** and **4** (at 610 nm) monitoring the PDI emission gave bi-exponential decays. The major (95–99 %) short components (9–54 ps) as well as the energy-transfer rates (k_{en}) derived are given in Table 3.

Figure 6 shows the decay traces of the four C_{60}–PDI systems. Interestingly, a minor long component (0.2–4 %, 3–5 ns) is observed in the time-resolved emission.[61] Table 3 shows the mono-exponential fluorescence lifetimes of the reference compounds **7**, **10**, and **14**. The lifetimes are virtually independent of deaerating and are in accordance with reported lifetimes for similar systems.[27,53,55–57,62]

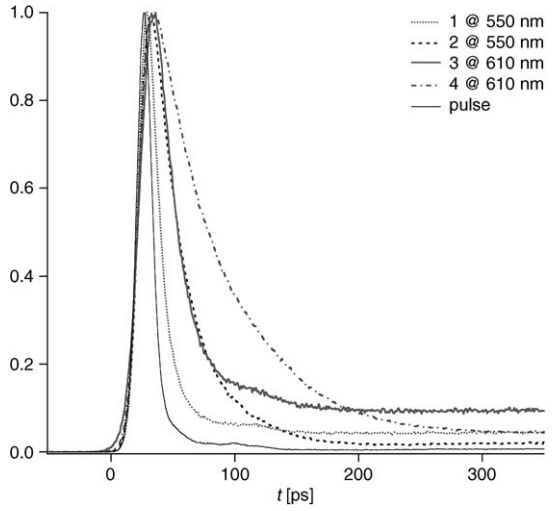

Figure 6. Emission decay traces obtained with SPC of compounds **1**–**4** in toluene. Pulse is also shown (λ_{ex} = 324 nm, 17 ps FWHM, detection wavelength is indicated).

By using the quenched lifetimes and applying $k_{en} = 1/\tau - 1/\tau_0$, singlet energy-transfer rates of $11.1 \times 10^{10}\ s^{-1}$ (for **1**), $3.3 \times 10^{10}\ s^{-1}$ (for **2**), $3.9 \times 10^{10}\ s^{-1}$ (for **3**), and $1.8 \times 10^{10}\ s^{-1}$ (for **4**) were obtained (Table 3). This correlates reasonably well with the rates that can be deduced from the steady-state data (Table 3). From these data it is already clear that the rate of energy transfer is modulated both by the bay substituent and by the spacer length. The shortest spacers display the faster rates. Considering the same spacer length, energy transfer is more efficient for the chlorinated than for the *tert*-butylphenoxy-substituted dyads. It can be noted that the energy-transfer rates obtained for dyads **1**–**4** are higher than those reported in the literature for other C_{60} fullerene-based dyads.[14,15,41,63]

Femtosecond transient absorption:[64] Femtosecond transient absorption was used to get more accurate information on

the singlet and triplet energy-transfer processes in the dyads. The spectral data obtained for **2** in toluene are shown in Figure 7. The typical bands of the PDI moiety, such as the ground-state bleaching (at 500 and 525 nm), the singlet-state emission (at ca. 600 nm), the singlet-excited-state absorption (at ca. 800 nm), and the triplet-excited-state absorption (at ca. 560 nm) are observed, similar to those reported before for **1**.[65] The kinetics of **2**, however, are different, showing a slower decay of the PDI excited-singlet state and a slower rise of the 560 nm band. For all dyads (**1**–**4**) the singlet excited state of the fullerene adduct is observed as an intermediate state (at 80 ps for **2**, see Figure 7A). Its absorption is rather weak and covers the whole visible range, with a minimum at around 600 nm.[65,66]

Overall, the phenoxy-substituted compounds **3** and **4** display similar behavior to **1** and **2**, but the spectral features of the PDI singlet and triplet excited states are different (Figure 8), especially the modulation by the strong ground-state bleaching at 580 nm for **3** and **4**. The phenoxy-substituted PDI moiety shows ground-state bleaching (at 540 and 580 nm), the singlet-state emission (at ca. 600 and 650 nm), and a weak singlet excited-state absorption (at ca. 700 nm). The final state populated (the triplet of PDI) is characterized by maxima at 510, 550 and by the strong bleach at 580 nm and an almost flat absorption band between 600 and 800 nm. Again, the dyad with the longer spacer (**4**) shows slower singlet and triplet energy transfer. Table 6 summarizes the characteristic times observed with femtosecond transient absorption for the dyads **1** to **4** in toluene. See Supporting Information for corresponding rates.

Table 6. Decay and rise times observed for dyads **1**–**4** in toluene with femtosecond transient absorption spectroscopy, corresponding to singlet–singlet energy transfer (τ_1, τ_2) and triplet–triplet energy transfer (τ_3).

	τ_1 [ps]	τ_2 [ps]	τ_3 [ns]
1	0.4	5	0.8
2	4.5	27	6.2
3	0.8	12	2.7
4	7	50	9

Interestingly, the ultrafast component observed in the femtosecond transient absorption spectroscopy is not detected with SPC, due to its lower time resolution. The slower components (τ_2) are in reasonable agreement with the fluorescence emission lifetimes (Table 3).

Femtosecond transient absorption spectroscopy was also performed in benzonitrile for compounds **1** and **3** to assess solvent-dependent photophysical behavior (i.e., the occurrence of electron transfer). Very similar spectral features were observed as well, as slightly different kinetics (see Supporting Information), the latter being attributed to small differences in solvent-dependent conformations resulting in slightly altered interchromophoric distances in the two solvents for the extended and folded forms. This clearly indicates that a charge-transfer state is not formed (or has no population build-up). Furthermore, the singlet energy transfer from the PDI to the C_{60} unit and subsequent triplet energy transfer from the fullerene triplet state to the perylene-based triplet are relatively insensitive to the solvent polarity.

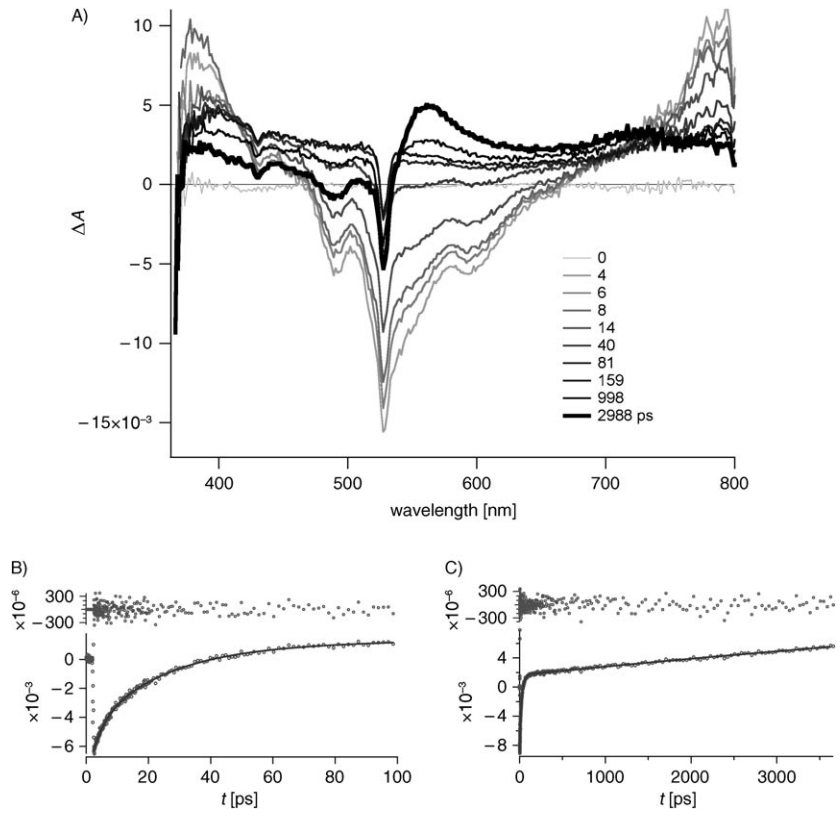

Figure 7. A) Femtosecond transient absorption spectra of compound **2** in toluene (λ_{ex} = 530 nm, 150 fs FWHM); kinetic traces B) at 600 nm on a 100-ps timescale and C) at 560 nm on the full timescale with tri-exponential fit (τ_1 = 4.5 ps, τ_2 = 27 ps, and τ_3 = 6.2 ns). Incremental time delays are indicated in A).

The femtosecond spectroscopy confirms that light energy harvested by the PDI antenna is transferred very efficiently to the C_{60} moiety on a (sub)picosecond (for **1**) to tens-of-picosecond timescale and that no electron transfer occurred between PDI and C_{60} moieties. No spectral features attributable to either the PDI radical anion or cation,[67] or the C_{60} radical cation[68] or anion[69] were observed. Using NIR detection, compounds **1** and **3**

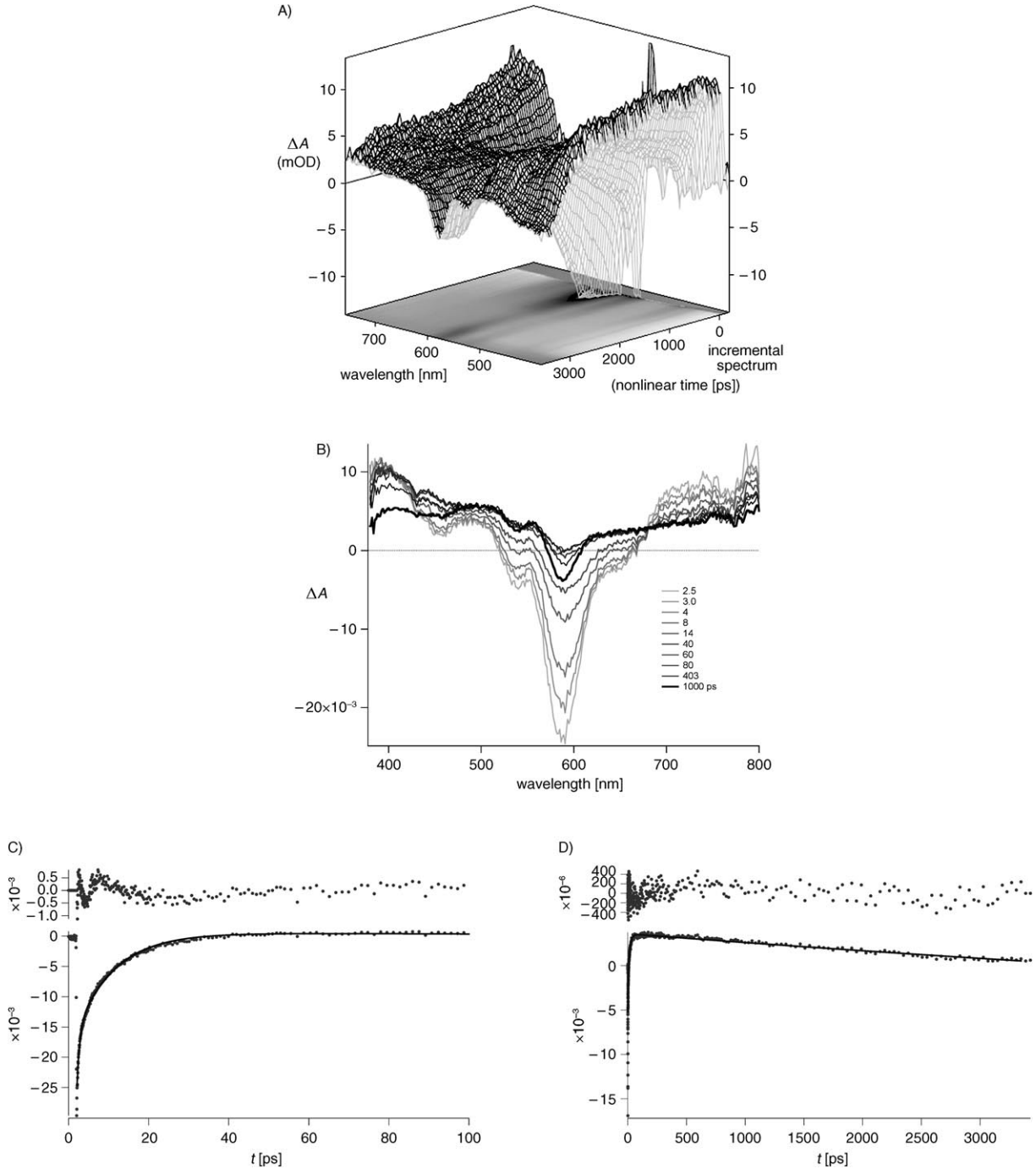

Figure 8. A) 3D surface plot of the femtosecond transient absorption data obtained for **3** in toluene ($\lambda_{ex}=530$ nm, 150 fs FWHM). Signal intensity is also projected on the *x*-*y* plane. The incremental time delay is short (0.04 ps) at the start and longer (50 ps) at later times (total timescale −10 to 3600 ps). Note that the time increases to the front and the wavelength increases to the left. B) Femtosecond transient absorption spectra of compound **3**. Incremental time delays are indicated in the legend of (B). Kinetic traces at 600 nm (C) and at 500 nm (D) together with tri-exponential fit ($\tau_1=0.8$ ps, $\tau_2=12$ ps, and $\tau_3=2.7$ ns).

show only singlet–singlet absorption in toluene[41h] at 990 nm for **1** and at 960 and 1040 nm for **3** (see Supporting Information) with kinetics similar to the singlet excited-state kinetics observed with the femtosecond transient absorption data using visible-light detection. Moreover, the final excited state is a low-energy (1.2 eV) triplet state localized on the PDI,[53] normally rarely observed in perylene dyes. Two rates of fast singlet energy transfer are observed, which were attributed to the co-existence of a folded and an extended conformer. The two faster rates observed with transient ab-

sorption show that the interchromophoric distance in the folded conformer of **2** and **4** is longer than for **1** and **3**, in agreement with DFT and Hartree–Fock calculations.[48]

Nanosecond transient absorption: The ultrafast spectroscopy described in the previous section clearly shows the formation of a longer-lived triplet state that is localized on the PDI unit in all four dyads. The triplet–triplet absorption spectra of the PDI chromophores observed with nanosecond transient absorption spectroscopy are given in Figure 9. The similarity to the final femtosecond transients (at 3.6 ns) is perfect. Tetrachloro-substituted PDI (**1** and **2**) are characterized by a very strong triplet-excited state absorption at 560 nm. Ground-state bleaching features are observed at 490 and 525 nm. Tetra-*tert*-butylphenoxy-substituted PDI (**3** and **4**) show a markedly different spectrum, due to the strong ground-state bleaching at 580 nm, characterized by maxima at 510 and 550 nm (for the spectra in benzonitrile, see Supporting Information). The observed triplet-state lifetimes in air and under deaerated conductions are given in Table 7. Notably, the lifetimes under degassed conditions

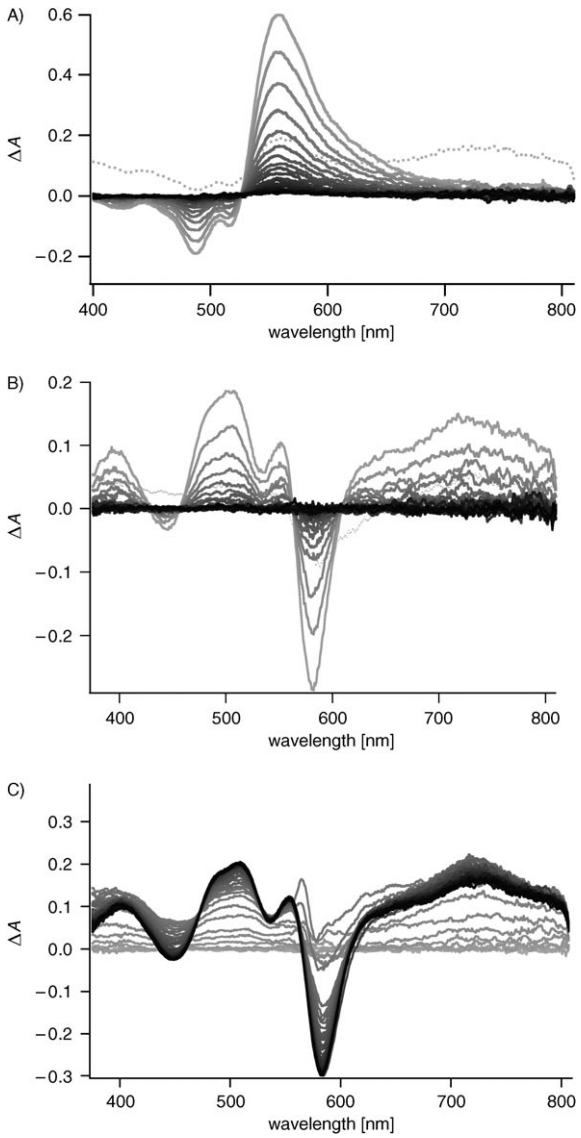

Figure 9. Nanosecond transient absorption spectra of the triplet state in toluene of A) compound **2**, incremental time delay is 2500 ns (argon degassed); B) compound **3**, incremental time delay is 120 ns non-degassed; C) compound **4**, incremental time delays is 1 ns. The first spectrum is dotted in A) and B) (time increases from grey to black). A) and B) present the decay of the PDI triplets. In B) some triplet C_{60} is observed at 710 nm. This 710 nm band shows a different decay behavior in (C), in which also the rise of the PDI triplet can be observed. For C) the time zero was chosen slightly before the laser pulse.

Table 7. Triple-state lifetimes of compounds **1**–**4** in toluene (tol) and benzonitrile (PhCN) under aerated (air) and de-aerated (Ar) conditions as observed by using nanosecond transient absorption spectroscopy.

	τ [ns, tol, air]	τ [ns, tol, Ar]	τ [ns PhCN, air]	τ [ns, PhCN, Ar]
1	440	12000	640	15000
2	400	10000	590	14000
3	330	14000	680	14000
4	310	15000	590	20000

are very sensitive to traces of oxygen left in solution and are influenced by triplet–triplet annihilation (and can thus be considered lower limits). The effects of de-oxygenation and comparison of the spectral shape with literature data[53,70] clearly show the nature of the PDI-localized triple state.[71]

The spectroscopy of compound **1** does not reveal any indication of C_{60} triplet-state formation in the femtosecond and nanosecond transient absorption, and its intermediacy is inferred from the intrinsic fullerene properties. This is different, however, for compound **4**. Figure 9C shows the clear kinetic difference for the 500 and 710 nm bands in the first 50 ns (Supporting Information Figure S6 for spectra of **1** and **2**). From these data an initial rise time of 9 ns is deduced (at 500 nm), which corresponds to the triplet energy transfer from C_{60} to the PDI. Now, a second, slower triplet energy transfer (in 33 ns) is inferred from the decay at 710 nm. A rise time at 500 nm is not observed due to overlapping bands and the small yield of this slower process. However, in a large part of the population of excited-state molecules, the fullerene triplet does not transfer its energy and decays with a lifetime very similar to that of the PDI triplet (Table 7). Clearly, the two conformations deduced from two singlet energy-transfer rates in the femtosecond transient now also give two different triplet energy-transfer rates.

Similar observations were made for compound **3**, for which the 710 nm band is clear in the nanosecond transient. Closer inspection of Figure 7 also reveals a spectroscopic sign for $^3C_{60}$ formation in compound **2**, by the small hump at 710 nm in the last trace (at 2988 ps). In the nanosecond transient, however, this appears to be masked by the strong and more red-shifted ^{3}PDI absorption (Figure 9). The feature at 710 nm is also not observed for compound **1**.[65]

For comparison and completeness the triplet–triplet absorption spectra[72] of the methanofullerene adduct **14** and

pristine C_{60} are given in the Supporting Information. The singlet–singlet absorption of **7** was reported previously.[65]

Quantum yields of triplet PDI formation were estimated by using the comparative method[73] and molar-absorption coefficients.[53,66] From this analysis we estimate that Φ_T (**1**) = 0.75, Φ_T (**2**) = 0.70 and Φ_T (**3**) = 0.60, Φ_T (**4**) = 0.52. The molar-absorption coefficients of the transient triplet species were estimated by using the iso-absorptive points[53] (Supporting Information). The observed triplet absorption spectrum has a maximum at 510 nm ($\varepsilon_{(T1-Tn)} = 9400\ M^{-1}\ cm^{-1}$) for compounds **3** and **4**. The observed triplet absorption spectra of **1** and **2** have a maximum at 560 nm ($\varepsilon_{(T1-Tn)} = 51\,600\ M^{-1}\ cm^{-1}$).

We can now assess the energetic scheme reported in Figure 10 for dyad **1**. Excitation at 520 nm, at which the PDI moiety selectively absorbs, leads to the population of singlet state centered on PDI. ^{1}PDI*–C_{60} decays by very fast energy transfer to form PDI–$^1C_{60}$* for which two rates are observed, attributed to a folded and an extended conformation. Fluorescence emission is more than 99% quenched. A charge-separated state PDI^-–C_{60}^+ is not populated, although its energy level is intermediate (Table 4). Clearly, singlet energy transfer is much faster. The final triplet state ^{3}PDI*–C_{60} is populated in high yield. Although the triplet state PDI–$^3C_{60}$* is not observed for dyad **1**, it is clearly observed for dyads **2**–**4**. Thus, it is clear that intersystem crossing from PDI–$^1C_{60}$* to PDI–$^3C_{60}$* precedes the energy transfer to the final PDI triplet state. Indeed, intersystem crossing is known to be very efficient for most mono-functionalized C_{60} derivatives (Φ_T close to unity, $\tau_f \approx 1.5$ ns and $\Phi_f \approx 5 \times 10^{-4}$) such as **14** and other compounds described in the literature.[55,57,72,74]

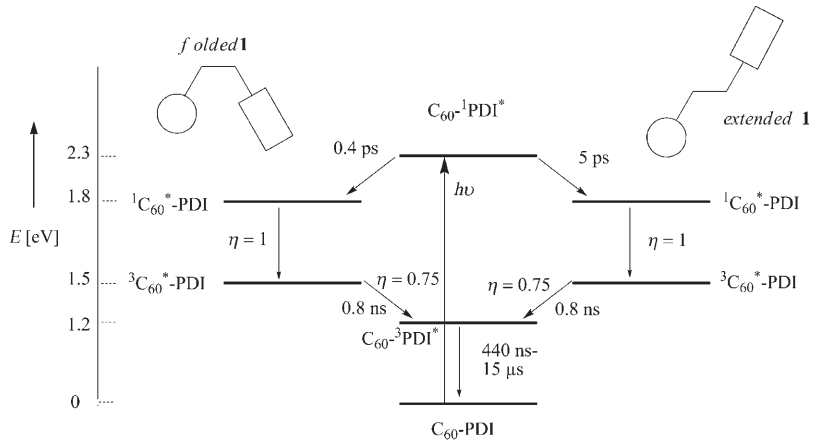

Figure 10. Energy-level diagram (on eV scale) showing the processes that take place in the two conformations of dyad **1** upon selective excitation of PDI moiety (toluene, RT). Lifetimes and efficiencies are also indicated.

Conclusion

Novel [60]fullerene–perylenediimide (C_{60}–PDI) dyads were developed as efficient light-harvesting systems designed for directional energy transfer. The PDI was introduced to play the role of a visible-light antenna, and after excitation of this PDI moiety in the dyads, we could prove a quantitative intramolecular energy transfer (>99%) from the PDI donor to the C_{60} acceptor. A Förster-type mechanism is suggested to explain this singlet–singlet energy transfer and it was demonstrated that the final populated excited state is a low-energy triplet state localized on the PDI moiety.

Interestingly, various intramolecular energy-transfer rates[41h,65] between C_{60} and different PDI-containing chloro-, phenoxy-, and pyrrolidino-substitutents at the bay position (the *orange*, *red*, and *green* PDI family[75]) at different molecular configurations are now available, making an extensive comparison of factors influencing the rates possible (see Supporting Information). It can already be noted that the combination of the *green* PDI with C_{60} through a pyrrolidine bridge results in much slower singlet and triplet energy transfer[41h] (in toluene), not only due to the restricted conformational freedom, but also to the much less favorable Förster overlap. This would imply that these types of NIR-absorbing imide dyes (that can harvest more of the sunlight) should be designed to display Dexter-type energy transfer.

It was also shown in these C_{60}–PDI dyads that the position of the first reduction potential of the PDI moiety in solution relative to this of C_{60} can be finely tuned by molecular engineering around the PDI bay region. This electrochemical parameter was correlated with preliminary results obtained from the conception of photovoltaic devices. These were tested by blending P3HT with C_{60}–PDI dyad and it was clearly evidenced in agreement with absorption and electrochemical properties that better photovoltaic characteristics were obtained with dyad **3** than with dyad **1**.[76] Further investigation concerning the incorporation of these dyads in photovoltaic devices is underway: firstly, the possibility of using the C_{60}–PDI dyad associated in variable amounts with [60]PCBM in the photoactive layer and secondly, the design of new light-harvesting dyads in which the first reduction process should be more selective between the two units.

Experimental Section

Materials and methods: Reagents were obtained commercially and were used without any purification. Fullerene C_{60} (99.5+%) was purchased from MER Corporation Fullerenes. 1,6,7,12-Tetrachloroperylenetetracarboxylic dianhydride **5** was furnished by BASF-AG (Ludwigshafen, Germany). Dry solvents were obtained by distillation over suitable dessicants (THF and toluene from Na/benzophenone, CH_2Cl_2 from P_2O_5, CH_3CN

from CaH_2). Thin-layer chromatography (TLC) was performed on aluminium sheets coated with silica gel 60F254. Column chromatography was carried out on silica gel (Kieselgel 60 Merck 5–40 μm).

The HPLC system consisted of a series of a model Waters 501 pump, a model Waters 2487 UV/Vis detector. Analytical separation was accomplished at 25 °C on a 250 mm × 4.6 mm ID column packed with a 5 μm AIT Kromasil Silica stationary phase. Semi-preparative separation was accomplished at 25 °C on a 250 mm × 10 mm column packed with a 5 μm AIT Kromasil Silica stationary phase. The operating conditions for the semi-preparative separation were a flow-rate of 1.5 mL min^{-1} (for **10**), 2 mL min^{-1} (for **4**, **7**, **14**), or 3 mL min^{-1} (for **1**, **2**, **3**), a mobile phase of toluene/CH_2Cl_2 (3:1, v/v) (for dyads **1**–**4** and **7**) or CH_2Cl_2 (for **10** and **14**) (HPLC grade Fisher Scientific). The injected solution was composed of 15 mg of compound in 2 mL of solvent. Detection was achieved at the absorbance of 335 nm (for **14**), 520 nm for **1**, **2**, **7**), or 580 nm (for **3**, **4**, **10**).

Melting points were determined by using a microscope with a Köfler hot stage and are uncorrected. ^{1}H (500 MHz) and ^{13}C (125 MHz) NMR spectra were recorded on a Bruker Avance DRX 500 spectrometer. Chemical shifts are reported as δ values in ppm using $CHCl_3$ as the reference. Infra-red spectra were obtained on a BIO-RAD FTS 155 spectrometer and UV/Vis experiments were performed on a Perkin–Elmer Lambda 19 NIR spectrometer. Mass spectra were recorded on a MALDI-TOF Bruker Biflex III. Elemental microanalyses were performed by the CNRS Central Service of Microanalysis (Vernaison, France).

Cyclic voltammetry was performed in a three-electrode cell equipped with a platinum millielectrode and a platinum wire counterelectrode. A silver wire served as quasi-reference electrode and its potential was checked against the ferricinium/ferrocene couple (Fc^+/Fc) before and after each experiment. The electrolytic media involved CH_2Cl_2 (HPLC grade), *o*-dichlorobenzene (Aldrich spectroscopic grade), and 0.1 M of tetrabutylammonium hexafluorophosphate (TBAHP, puriss quality). All experiments were performed in a glove box containing dry, oxygen-free (<1 ppm) argon, at RT. Electrochemical experiments were carried out using an EGG PAR 273A potentiostat.

Electronic absorption spectra were recorded on a Lambda 19 NIR model from Perkin–Elmer. Fluorescence spectra were recorded in non-deoxygenated solvents (spectroscopic grade) at 20 °C with a QM-4/QuantaMaster fluorometer from PTI equipped with rapid monochannel detection and continuous excitation source. Quantum yields were determined using cresyl violet as a standard reference ($\Phi_f = 0.54$ at 20 °C in MeOH).

For time-resolved spectroscopy, samples were dissolved in spectroscopic solvents (toluene and benzonitrile from Aldrich) and filtered (0.4 μm PVDF HPLC filters) to remove particles and potential aggregates. The samples had an absorbance of ca. 0.7–0.9 (1 cm) for nanosecond transient measurements and of ca. 0.3–0.7 (2 mm) for femtosecond transient at the excitation wavelength. The UV/Vis absorption spectra of the samples were measured before and after the laser experiments and were found to be virtually identical, thus ruling out any possible degradation or chemical change in the samples. All photophysical data reported here have an error limit of 5–10 %, unless indicated otherwise. The experiments were performed at RT.

Femtosecond transient absorption experiments were performed with a Spectra-Physics Hurricane Titanium:Sapphire regenerative amplifier system. The full spectrum setup was based on an optical parametric amplifier (Spectra-Physics OPA 800C) as the pump. The residual fundamental light, from the pump OPA, was used for white-light generation, which was detected with a CCD spectrograph (Ocean Optics). The polarization of the pump light was controlled by a Berek Polarization Compensator (New Focus). The Berek Polarizer was always included in the setup to provide the Magic-Angle conditions. The probe light was double-passed over a delay line (Physik Instrumente, M-531DD) that provides an experimental time window of 3.6 ns with a maximal resolution of 0.6 fs per step. The OPA was used to generate excitation pulses at 530 nm. The laser output was typically 3.5–5 μJ pulse^{-1} (130 fs FWHM) with a repetition rate of 1 kHz. The samples were placed into cells of 2 mm path length (Hellma) and were stirred with a downward projected PTFE shaft using a direct-drive spectro-stir (SPECTRO-CELL). This stir system was also used for the white-light generation in a 2 mm water cell. For femtosecond transient absorption in the NIR region a Control Development NIR-256L-1.7T1-USB optical spectrometer system, InGaAs detector with 512 element arrays responding to wavelengths range from 900–1700 nm was used. Detection light was generated with a sapphire plate.

Time-resolved fluorescence measurements were performed using a picosecond single-photon counting (SPC) setup. The frequency-doubled (300–340 nm, 1 ps, 3.8 MHz) output of a cavity-dumped DCM dye laser (Coherent model 700) pumped by a mode-locked Ar-ion laser (Coherent 486 AS Mode Locker, Coherent Innova 200 laser) was used as the excitation source. A (Hamamatsu R3809) microchannel-plate photomultiplier was used as detector. The instrument response (≈17 ps FWHM) was recorded using the Raman scattering of a doubly de-ionized water sample. Time windows (4000 channels) of 5 ns (1.25 ps/channel) to 50 ns (12.5 ps/channel) could be used, enabling the measurement of lifetimes of 5 ps–40 ns. The recorded traces were deconvoluted with the system response and fitted to an exponential function using the Igor Pro program.

In nanosecond pump-probe experiments, a (Coherent) Infinity Nd:YAG-XPO laser was used for excitation. The laser illuminated a slit of 10 × 2 mm. Perpendicular to this, the probe light was provided by an EG&G (FX504) low-pressure Xenon lamp that irradiated the sample through a 1 mm pinhole. The overlap of the two beams falls within the first two millimeters of the cell, after the slit. The probe light from both the signal and the reference channels is then collected in optical fibers that are connected to an Acton SpectraPro-150 spectrograph that is coupled to a Princeton Instruments ICCD-576-G/RB-EM gated intensified CCD camera. Using a 5 ns gate this camera simultaneously records the spectrally dispersed light from both optical fibers on separate stripes of the CCD. Deaeration was performed by bubbling with Argon for 20 to 30 min.

Dyad 1: To a solution of **12a** (189 mg, 0.25 mmol) in anhydrous toluene (80 mL) were added successively C_{60} (360 mg, 0.50 mmol), iodine (94 mg, 0.37 mmol), and DBU (85 μL, 0.57 mmol). The reaction mixture was stirred at RT under nitrogen for 3 h. After addition of water (50 mL), the resulting emulsion was extracted with CH_2Cl_2 (3 × 30 mL). The combined organic phases were washed with 1 N HCl (2 × 50 mL), water (2 × 50 mL), dried over $MgSO_4$ and concentrated under reduced pressure. The residue was purified by column chromatography on silica gel by using CS_2 to remove unreacted C_{60}, then CH_2Cl_2/EtOAc 9:1. A second column chromatography on silica gel was performed by using toluene/EtOAc 95:5. Recrystallization using CH_2Cl_2/petroleum ether afforded pure dyad **1** as a red powder (195 mg; 53 %). ^{1}H NMR ($CDCl_3$): $\delta = 8.66$ (s, 2H), 8.63 (s, 2H), 5.09 (ddd, $^3J = 3.5$, $^3J = 8.5$ Hz, $^2J = 14$ Hz, 1H), 4.92 (ddd, $^3J = 3.5$, $^3J = 8.5$ Hz, $^2J = 14$ Hz, 1H), 4.78 (ddd, $^3J = 3.5$, $^3J = 8.5$ Hz, $^2J = 14$ Hz, 1H), 4.62 (ddd, $^3J = 3$, $^3J = 3.5$, $^3J = 8.5$ Hz, $^2J = 14$ Hz, 1H), 4.57 (q, $^3J = 7$ Hz, 2H), 4.20 (t, $^3J = 7$ Hz, 2H), 1.75 (m, 2H), 1.50 (t, $^3J = 7$ Hz, 3H), 1.42 (m, 4H), 0.94 ppm (t, $^3J = 7$ Hz, 3H); ^{13}C NMR ($CDCl_3$): $\delta = 163.82$, 163.21, 162.26, 162.19, 145.15, 145.11, 145.05, 145.00, 144.96, 144.81, 144.75, 144.66, 144.57, 144.55, 144.51, 144.44, 144.42, 144.40, 144.25, 144.16, 143.76, 143.66, 143.15, 142.96, 142.89, 142.84, 142.79, 142.76, 142.74, 142.65, 142.32, 142.06, 141.98, 141.80, 141.74, 141.63, 141.50, 141.00, 140.87, 140.83, 140.58, 139.87, 138.91, 138.54, 138.46, 135.58, 135.45, 133.44, 132.98, 131.39, 131.21, 128.89, 128.30, 123.38, 123.21, 122.54, 71.31, 71.30, 63.75, 63.57, 51.97, 40.98, 39.12, 29.15, 27.76, 22.41, 14.26, 13.99 ppm; IR (KBr): $\tilde{\nu} = 1747$, 1705, 1667, 1589, 1236, 527 cm^{-1}; MS (MALDI-TOF, pos. mode, dithranol): *m*/*z*: calcd for: 1472.03; found: 1472.07 $[M]^{+\bullet}$; elemental analysis calcd (%) for $C_{96}H_{24}Cl_4N_2O_8$ (1475.04): C 78.17, H 1.64; found: C 77.91, H 1.92.

Dyad 2: To a solution of **12b** (120 mg, 0.15 mmol) in anhydrous toluene (50 mL) were added successively C_{60} (216 mg, 0.30 mmol), iodine (58 mg, 0.23 mmol), and DBU (50 μL, 0.33 mmol). The reaction mixture was stirred at RT under nitrogen for 4 h. After addition of water (50 mL), the resulting emulsion was extracted with CH_2Cl_2 (3 × 30 mL). The combined organic phases were washed with 1 N HCl (50 mL), water (2 × 50 mL), dried over $MgSO_4$ and concentrated under reduced pressure. The residue was purified by column chromatography on silica gel by using CS_2 to remove unreacted C_{60}, then petroleum ether/CH_2Cl_2 3:7. Recrystallization using CH_2Cl_2/petroleum ether afforded pure dyad **2** as a red powder

(96 mg; 42%). ^{1}H NMR ($CDCl_3$): δ = 8.67 (s, 2H), 8.66 (s, 2H), 4.60–4.50 (m, 2H), 4.55 (q, ^3J = 7 Hz, 2H), 4.26 (t, ^3J = 7 Hz, 2H), 4.21 (t, ^3J = 7 Hz, 2H), 1.94 (quint, ^3J = 7.5 Hz, 2H), 1.87 (quint, ^3J = 7.5 Hz, 2H), 1.75 (quint, ^3J = 7.5 Hz, 2H), 1.64 (quint, ^3J = 7.5 Hz, 2H), 1.50 (t, ^3J = 7 Hz, 3H), 1.45–1.40 (m, 4H), 0.94 ppm (t, ^3J = 7 Hz, 3H); IR (KBr): $\tilde{\nu}$ = 1744, 1703, 1665, 1587, 525 cm^{-1}; MS (MALDI-TOF, pos. mode, dithranol): *m*/*z*: calcd for: 1514.08; found: 1512.95 $[M-H]^+$; elemental analysis calcd (%) for $C_{99}H_{30}Cl_4N_2O_8$ (1517.12): C 78.38, H 1.99; found: C 76.98, H 2.38.

Dyad 3: To a solution of **13a** (363 mg, 0.3 mmol) in anhydrous toluene (100 mL) were added successively C_{60} (432 mg, 0.6 mmol), iodine (114 mg, 0.45 mmol), and DBU (102 μL, 0.68 mmol). The reaction mixture was stirred at RT under nitrogen for 4 h. After addition of water (50 mL), the resulting emulsion was extracted with CH_2Cl_2 (3×60 mL). The combined extracts were washed with washed with 1N HCl (2× 50 mL), water (2×50 mL), dried over $MgSO_4$ and concentrated under reduced pressure. The residue was purified by column chromatography on silica gel by using CS_2 to remove unreacted C_{60}, then CH_2Cl_2/EtOAc 9:1. A second column chromatography on silica gel using petroleum ether/CH_2Cl_2 3:7 was performed. Recrystallization using CH_2Cl_2/petroleum ether afforded pure dyad **3** as a purple powder (270 mg; 47%). ^{1}H NMR ($CDCl_3$, 298 K): δ = 8.19 (s, 2H), 8.15 (s, 2H), 7.18 and 7.17 (2d, ^3J = 8.6 Hz, 8H), 6.75 and 6.73 (2d, ^3J = 8.6 Hz, 8H), 4.90 (brs, 1H), 4.82 (brs, 1H), 4.72 (brs, 1H), 4.64 (brs, 1H), 4.50 (q, ^3J = 7 Hz, 2H), 4.09 (t, ^3J = 7.5 Hz, 2H), 1.66 (brt, 2H), 1.43 (t, ^3J = 7 Hz, 3H), 1.27 (s, 36H), 1.23–1.36 (m, 4H), 0.88 ppm (t, ^3J = 7 Hz, 3H); the ^{1}H NMR recorded in $CDCl_3$ at 343 K presents two signals at 4.86 (brs, 2H) and 4.67 ppm (brs, 2H) instead of the four broad signals at 5.09 (1H), 4.92 (1H), 4.78 (1H), 4.62 ppm (1H); ^{13}C NMR ($CDCl_3$): δ = 163.40, 163.33, 156.00, 155.80, 152.83, 152.71, 147.22, 147.18, 145.11, 144.98, 144.88, 144.75, 144.70, 144.50, 144.43, 143.73, 143.42, 142.77, 142.72, 141.99, 141.69, 139.49, 129.02, 128.21, 126.67, 126.63, 122.56, 121.75, 121.00, 120.22, 120.20, 119.83, 119.35, 119.30, 119.20, 77.57, 71.38, 63.63, 63.52, 52.19, 40.63, 38.37, 34.33, 31.43, 29.69, 29.19, 27.73, 22.35, 21.45, 14.15, 13.95 ppm; IR (KBr): $\tilde{\nu}$ = 2958, 1748, 1700, 1663, 1588, 1503, 1284, 526 cm^{-1}; MS (MALDI-TOF, pos. mode, dithranol): *m*/*z*: calcd for: 1928.54; found: 1928.52 $[M]^{+\bullet}$; elemental analysis calcd (%) for $C_{136}H_{76}N_2O_{12}$ (1930.06): C 84.63, H 3.97; found: C 82.90, H 4.25.

Dyad 4: To a solution of **13b** (150 mg, 0.12 mmol) in anhydrous toluene (30 mL) were added successively C_{60} (130 mg, 0.18 mmol), iodine (46 mg, 0.18 mmol), and DBU (54 μL, 0.36 mmol). The reaction mixture was stirred at RT under nitrogen for 48 h. The solvent was concentrated under reduced pressure and the residue was purified by column chromatography on silica gel using successively CS_2 to remove unreacted C_{60}, toluene/acetone 9:1, then petroleum ether/CH_2Cl_2 1:4. Recrystallization using CH_2Cl_2/petroleum ether afforded pure dyad **4** as a purple powder (120 mg; 51%). ^{1}H NMR ($CDCl_3$): δ = 8.22 (s, 2H), 8.19 (s, 2H), 7.22 and 7.21 (2d, ^3J = 9 Hz, 8H), 6.81 and 6.79 (2d, ^3J = 9 Hz, 8H), 4.50 (q, ^3J = 7 Hz, 2H), 4.49 (t, ^3J = 7 Hz, 2H), 4.15 (t, ^3J = 7 Hz, 2H), 4.10 (t, ^3J = 7 Hz, 2H), 1.86 (quint, ^3J = 7 Hz, 2H), 1.78 (quint, ^3J = 7 Hz, 2H), 1.68 (quint, ^3J = 7 Hz, 2H), 1.57 (m, 2H), 1.44 (t, ^3J = 7 Hz, 3H), 1.36 (m, 4H), 1.28 (s, 36H), 0.88 ppm (t, ^3J = 7 Hz, 3H); IR (KBr): $\tilde{\nu}$ = 2957, 1746, 1698, 1661, 1588, 1504, 1283, 526 cm^{-1}; MS (MALDI-TOF, pos. mode, dithranol): *m*/*z*: calcd for: 1970.59; found: 1970.29 $[M]^{+\bullet}$; elemental analysis calcd (%) for $C_{139}H_{82}N_2O_{12}$ (1972.1): C 84.65, H 4.19; found: C 83.35, H 4.35.

***N*-2′-Hydroxyethyl-*N*′-pentyl-1,6,7,12-tetrachloroperylene-3,4:9,10-bis(dicarboximide) (6a)**: To a solution of 1,6,7,12-tetrachloroperylene-3,4:9,10-tetracarboxylic dianhydride **5** (10 g; 18.9 mmol) in toluene (110 mL) were added simultaneously *n*-pentylamine (2.2 mL, 18.9 mmol) and ethanolamine (1.2 mL, 18.9 mmol). The reaction mixture was heated under reflux for 24 h and after cooling the solvent was concentrated under reduced pressure. The residue was extracted by using hot CH_2Cl_2 (10×100 mL) and the combined extracts were concentrated under reduced pressure. The residue was purified by column chromatography on silica gel. Symmetrical derivative **7** was first isolated by using CH_2Cl_2, then unsymmetrical compound **6a** was obtained as a red powder using CH_2Cl_2/EtOAc 4:1 (3.4 g, 28%). ^{1}H NMR ($CDCl_3$): δ = 8.62 (s, 2H), 8.60 (s, 2H), 4.50 (t, ^3J = 7.5 Hz, 2H), 4.30–4.10 (brs, 1H), 4.20 (t, ^3J = 7.5 Hz, 2H), 4.00 (t, ^3J = 7 Hz, 2H), 1.80 (m, 2H), 1.50 (m, 4H), 0.95 ppm (t, ^3J = 7.5 Hz, 3H); IR (KBr): $\tilde{\nu}$ = 3436 (br, OH), 1702, 1658, 1587 cm^{-1}; MS (MALDI-TOF, pos. mode, dithranol): *m*/*z*: calcd for: 640.01; found: 640.08 $[M]^{+\bullet}$; elemental analysis calcd (%) for $C_{31}H_{20}Cl_4N_2O_5$ (642.31): C 57.97, H 3.14, N 4.36; found: C 56.43, H 3.18, N 4.17.

***N*-2′-Hydroxypentyl-*N*′-pentyl-1,6,7,12-tetrachloroperylene-3,4:9,10-bis(dicarboximide) (6b)**: To a solution of 1,6,7,12-tetrachloroperylene 3,4:9,10-tetracarboxylic dianhydride **5** (10 g; 18.9 mmol) in toluene (110 mL) were added simultaneously *n*-pentylamine (2.2 mL, 18.9 mmol) and 5-aminopentanol (2.0 mL, 18.9 mmol). The reaction mixture was heated under reflux for 3 d and after cooling to RT the solvent was concentrated under reduced pressure. The residue was extracted by using CH_2Cl_2 (200 mL). The filtrate was concentrated under reduced pressure and the residue was purified by column chromatography on silica gel. Symmetrical derivative **7** was first isolated using CH_2Cl_2, then unsymmetrical compound **6b** was obtained as a red powder using CH_2Cl_2/EtOAc 4:1 (2.24 g, 17%). ^{1}H NMR ($CDCl_3$): δ = 8.68 (s, 2H), 8.67 (s, 2H), 4.24 (t, ^3J = 7 Hz, 2H), 4.21 (t, ^3J = 7 Hz, 2H), 4.20 (s, 1H), 3.69 (t, ^3J = 7 Hz, 2H), 1.80 (quint, ^3J = 7.5 Hz, 2H), 1.75 (quint, ^3J = 7.5 Hz, 2H), 1.68 (quint, ^3J = 7.5 Hz, 2H), 1.53 (quint, ^3J = 7.5 Hz, 2H), 1.42 (m, 4H), 0.93 ppm (t, ^3J = 7 Hz, 3H); IR (KBr): $\tilde{\nu}$ = 3407 (br, OH), 1703, 1665, 1588 cm^{-1}; MS (MALDI-TOF, pos. mode, dithranol): *m*/*z*: calcd for: 682.06; found: 682.03; elemental analysis calcd (%) for $C_{34}H_{26}Cl_4N_2O_5$ (684.39): C 59.67, H 3.83, N 4.09; found: C 59.33, H 3.92, N 4.01.

***N*,*N*′-Dipentyl-1,6,7,12-tetrachloroperylene-3,4:9,10-bis(dicarboximide) (7)**: Synthesis of this compound was described previously.[26b]

***N*-2′-Hydroxyethyl-*N*′-pentyl-1,6,7,12-tetra(*p*-tertiobutyl)phenoxyperylene-3,4:9,10-bis(dicarboximide) (9a)**: A mixture of perylenediimide **6a** (860 mg, 1.4 mmol), *p*-tertiobutylphenol (2.1 g, 14 mmol), and K_2CO_3 (2 g, 14.5 mmol) in *N*-methylpyrrolidone (NMP) (50 mL) was stirred at 130°C under nitrogen for 14 h. After being cooled to RT, the reaction mixture was poured into HCl acid (1N) (50 mL). The precipitate was collected by filtration, washed thoroughly with water until neutrality, then purified by column chromatography on silica gel using successively CH_2Cl_2 then CH_2Cl_2/acetone 30:1. Recrystallization from CH_2Cl_2/methanol afforded compound **9a** as a purple powder, which was washed with petroleum ether to remove traces of methanol (920 mg, 60%). ^{1}H NMR ($CDCl_3$, 500 MHz): δ = 8.24 (s, 2H), 8.22 (s, 2H), 7.25 (d, ^3J = 9 Hz, 8H), 6.80 (d, ^3J = 9 Hz, 8H), 4.40 (t, ^3J = 7 Hz, 2H,), 4.40–4.20 (brs, 1H), 4.10 (t, ^3J = 7 Hz, 2H), 3.93 (t, ^3J = 7 Hz, 2H), 1.70 (brt, 2H), 1.40–1.35 (m, 4H), 1.30 (s, 36H), 0.95 ppm (t, ^3J = 7 Hz, 3H); IR (KBr): $\tilde{\nu}$ = 3438 (br, OH), 1693, 1657, 1586, 1507, 1292 cm^{-1}; MS (MALDI-TOF, pos. mode, dithranol): *m*/*z*: calcd for: 1096.52; found: 1096.23 $[M]^{+\bullet}$; elemental analysis calcd (%) for $C_{71}H_{72}N_2O_9$ (1097.34): C 77.71, H 6.61, N 2.55; found: C 76.54, H 6.31, N 2.57.

***N*-2′-Hydroxypentyl-*N*′-pentyl-1,6,7,12-tetra(*p*-tertiobutyl)phenoxyperylene-3,4:9,10-bis(dicarboximide) (9b)**: A mixture of perylenediimide **6b** (68.5 mg, 0.1 mmol), *p*-tertiobutylphenol (150 mg, 1 mmol), and K_2CO_3 (143 mg, 1.05 mmol) in *N*-methylpyrrolidone (NMP) (5 mL) was stirred at 130°C under nitrogen for 1 h. After being cooled to RT, the reaction mixture was poured into HCl acid (1N) (15 mL). The precipitate was collected by filtration, washed thoroughly with water until neutrality, then purified by column chromatography on silica gel using successively CH_2Cl_2 then CH_2Cl_2/acetone 30:1. Recrystallization from CH_2Cl_2/methanol afforded compound **9b** as a purple powder which was washed with petroleum ether to remove traces of methanol (66 mg, 58%). ^{1}H NMR ($CDCl_3$, 500 MHz): δ = 8.22 (s, 4H), 7.23 (d, ^3J = 9 Hz, 8H), 6.83 and 6.82 (2d, ^3J = 9 Hz, 8H), 4.13 (t, ^3J = 7 Hz, 2H), 4.10 (t, ^3J = 7 Hz, 2H), 3.63 (t, ^3J = 7 Hz, 2H), 1.72 (quint, ^3J = 7.5 Hz, 2H), 1.67 (brt, ^3J = 7.5 Hz, 1H), 1.61 (quint, ^3J = 7.5 Hz, 2H), 1.44 (quint, ^3J = 7.5 Hz, 2H), 1.38–1.32 (m, 6H), 1.29 (s, 36H), 0.88 ppm (t, ^3J = 7 Hz, 3H); IR (KBr): $\tilde{\nu}$ = 3500 (br, OH), 2962, 1697, 1658, 1588, 1505, 1291 cm^{-1}; MS (MALDI-TOF, pos. mode, dithranol): *m*/*z*: calcd for: 1138.57; found: 1138.03 $[M]^{+\bullet}$; elemental analysis calcd (%) for $C_{74}H_{78}N_2O_9$ (1139.42): C 78.00, H 6.90, N 2.46; found: C 77.48, H 6.74, N 2.41.

***N*,*N*′-Dipentyl-1,6,7,12-tetra(*p*-tertiobutyl)phenoxyperylene-3,4:9,10-3,4:9,10-bis(dicarboximide) (10)**: A mixture of perylenediimide **7** (5 g,

7.5 mmol), *p*-tertiobuylphenol (11.3 g, 75 mmol), and K_2CO_3 (10.4 g, 75 mmol) in *N*-methylpyrrolidone (NMP) (160 mL) was stirred at 130 °C under nitrogen for 14 h. After being cooled to RT, the reaction mixture was poured into HCl acid (1 N) (40 mL). The precipitate was collected by filtration, washed thoroughly with water until neutrality, then purified by column chromatography on silica gel using CH_2Cl_2/acetone 30:1. Recrystallization from CH_2Cl_2/methanol afforded compound **10** as a purple powder, which was washed with petroleum ether to remove traces of methanol (5.8 g, 69 %). ^{1}H NMR ($CDCl_3$, 500 MHz): δ = 8.22 (s, 4H), 7.23 (d, ^3J = 9 Hz, 8H), 6.82 (d, ^3J = 9 Hz, 8H), 4.10 (t, ^3J = 7.5 Hz, 4H), 1.67 (quint, ^3J = 7.5 Hz, 4H), 1.34 (m, 8H), 1.29 (s, 36H), 0.88 ppm (t, ^3J = 7 Hz, 6H); IR (KBr): $\tilde{\nu}$ = 2956, 1706, 1659, 1590, 1497, 1289 cm^{-1}; MS (MALDI-TOF, pos. mode, dithranol): *m*/*z*: calcd for: 1122.58; found: 1122.02 $[M]^{+\bullet}$; elemental analysis calcd (%) for $C_{74}H_{78}N_2O_8$ (1123.42): C 79.11, H 7.00, N 2.49; found: C 78.76, H 7.01, N 2.41.

Ethyl 2-*N*-(*N*′-pentyl-1,6,7,12-tetrachloroperylene-3,4:9,10-3,4:9,10-bis(dicarboximide)ethyl malonate (12a): To a solution of alcohol **6a** (193 mg, 0.3 mmol) in anhydrous CH_2Cl_2 (50 mL) were added successively at 0 °C under nitrogen fresh pyridine (77 μL, 0.94 mmol) and ethyl malonyl chloride 90 % (130 μL, 0.92 mmol). The reaction mixture was refluxed for 1 h. After cooling to RT, the solvent was concentrated under reduced pressure. The residue was purified by column chromatography on silica gel using CH_2Cl_2/EtOAc 4:1. Recrystallization from CH_2Cl_2/petroleum ether afforded compound **12a** as a red powder (210 mg, 93 %). ^{1}H NMR ($CDCl_3$, 500 MHz): δ = 8.69 (s, 2H), 8.68 (s, 2H), 4.55 (s, 4H), 4.21 (br t, ^3J = 7.5 Hz, 2H), 4.13 (q, ^3J = 7 Hz, 2H), 3.36 (s, 2H), 1.75 (quint, ^3J = 7.5 Hz, 2H), 1.44–1.39 (m, 4H), 1.23 (t, ^3J = 7.5 Hz, 3H), 0.93 ppm (t, ^3J = 7 Hz, 3H); ^{13}C NMR ($CDCl_3$): δ = 166.62 (C=O ester), 166.24 (C=O ester), 162.38 (C=O imide), 162.21 (C=O imide), 135.46, 135.30, 133.08, 132.94, 131.44, 131.40, 128.85, 128.47, 123.36, 123.31, 123.25, 122.84, 62.45, 61.54, 41.36, 40.93, 39.40, 29.13, 27.75, 22.40, 14.02, 13.97 ppm; IR (KBr): $\tilde{\nu}$ = 1764, 1744, 1706, 1667, 1594 cm^{-1}; MS (MALDI-TOF, pos. mode, dithranol): *m*/*z*: calcd for: 754.04; found: 753.97 $[M]^{+\bullet}$; elemental analysis calcd (%) for $C_{36}H_{26}Cl_4N_2O_8$ (756.41): C 57.16, H 3.46, N 3.70; found: C 56.34, H 3.59, N 3.55.

Ethyl 2-*N*-(*N*′-pentyl-1,6,7,12-tetrachloroperylene-3,4:9,10-bis(dicarboximide)pentyl malonate (12b): To a solution of alcohol **6b** (200 mg, 0.29 mmol) in anhydrous CH_2Cl_2 (40 mL) were added successively at 0 °C under nitrogen fresh pyridine (0.1 mL, 1.22 mmol) and ethyl malonyl chloride 90 % (0.13 mL, 0.89 mmol). The reaction mixture was refluxed for 2 h. After cooling to RT, the solvent was concentrated under reduced pressure. The residue was purified by column chromatography on silica gel using CH_2Cl_2/EtOAc 95:5. Recrystallization from CH_2Cl_2/methanol afforded compound **12b** as a red powder, which was washed with petroleum ether to remove traces of methanol (220 mg, 94 %). ^{1}H NMR ($CDCl_3$, 500 MHz): δ = 8.69 (s, 2H), 8.68 (s, 2H), 4–24–4.19 (m, 6H), 4.19 (q, ^3J = 7 Hz, 2H), 3.38 (s, 2H), 1.82–1.74 (m, 4H), 1.65–1.38 (m, 6H), 1.51 (m, 2H), 1.28 (t, ^3J = 7 Hz, 3H), 0.93 ppm (t, ^3J = 7 Hz, 3H); IR (KBr): $\tilde{\nu}$ = 1734, 1704, 1665, 1588 cm^{-1}; MS (MALDI-TOF, pos. mode, dithranol): *m*/*z*: calcd for: 796.09; found: 795.89 $[M]^{+\bullet}$; elemental analysis calcd (%) for $C_{39}H_{32}Cl_4N_2O_8$ (798.49): C 58.66, H 4.04, N 3.51; found: C 57.86, H 3.52, N 3.47.

Ethyl 2-*N*-(*N*′-pentyl-1,6,7,12-tetra(*p*-tertiobutyl)phenoxy perylene-3,4:9,10-bis(dicarboximide)ethyl malonate (13a): To a solution of alcohol **9a** (134 mg, 0.12 mmol) in anhydrous CH_2Cl_2 (20 mL) were added successively at 0 °C under nitrogen fresh pyridine (35 μL, 1.22 mmol) and ethyl malonyl chloride 90 % (55 μL, 0.27 mmol). The reaction mixture was refluxed for 2 h. After cooling to RT, the solvent was concentrated under reduced pressure. The residue was purified by column chromatography on silica gel using CH_2Cl_2/EtOAc 9:1. Recrystallization from CH_2Cl_2/methanol afforded compound **13a** as a purple powder, which was washed with petroleum ether to remove traces of methanol (135 mg, 91 %). ^{1}H NMR ($CDCl_3$, 500 MHz): δ = 8.23 (s, 2H), 8.21 (s, 2H), 7.23 (d, ^3J = 9 Hz, 4H), 7.22 (d, ^3J = 9 Hz, 4H), 6.83 (d, ^3J = 9 Hz, 4H), 6.81 (d, ^3J = 9 Hz, 4H), 4.45 (s, 4H), 4.10 (d, ^3J = 7.5 Hz, 2H), 4.08 (q, ^3J = 7 Hz, 2H), 3.30 (s, 2H), 1.67 (quint, ^3J = 7.5 Hz, 2H), 1.37–1.33 (m, 4H), 1.29 (s, 36H), 1.17 (t, ^3J = 7 Hz, 3H), 0.87 ppm (t, ^3J = 7 Hz, 3H); ^{13}C NMR ($CDCl_3$): δ = 166.49, 166.27, 166.47, 163.42, 156.09, 155.78, 152.91, 152.76, 147.32, 147.26, 132.84, 126.67, 122.56, 122.01, 120.91, 120.25, 120.17, 119.75, 119.59, 119.37, 119.20, 77.59, 62.43, 61.49, 41.41, 40.62, 38.93, 34.37, 31.45, 29.18, 27.74, 22.36, 13.98 ppm; IR (KBr): $\tilde{\nu}$ = 2971, 1700, 1657, 1588, 1507, 1291 cm^{-1}; MS (MALDI-TOF, pos. mode, dithranol): *m*/*z*: calcd for: 1210.55; found: 1210.49 $[M]^{+\bullet}$; elemental analysis calcd (%) for $C_{76}H_{78}N_2O_{12}$ (1211.44): C 75.35, H 6.49, N 2.31; found: C 73.94, H 6.23, N 2.31.

Ethyl 2-(*N*,*N*′-pentyl-1,6,7,12-tetra(*p*-tertiobutyl)perylene-3,4:9,10-bis(dicarboximide)pentyl malonate (13b): To a solution of alcohol **9b** (300 mg, 0.26 mmol) in anhydrous CH_2Cl_2 (40 mL) were added successively at 0 °C under nitrogen fresh pyridine (0.17 mL, 2.1 mmol) and ethyl malonyl chloride 90 % (0.2 mL, 1.6 mmol). The reaction mixture was refluxed for 36 h. After cooling to RT, the solvent was concentrated under reduced pressure. Recrystallization from CH_2Cl_2/methanol afforded compound **13a** as a purple powder, which was washed with petroleum ether to remove traces of methanol (291 mg, 88 %). ^{1}H NMR ($CDCl_3$, 500 MHz): δ = 8.22 (s, 4H), 7.23 (d, ^3J = 9 Hz, 8H), 6.83 (d, ^3J = 9 Hz, 4H), 6.81 (d, ^3J = 9 Hz, 4H), 4.16 (q, ^3J = 7 Hz, 2H), 4.13–4.08 (m, 6H), 3.33 (s, 2H), 1.74–1.64 (m, 6H), 1.47–1.41 (m, 2H), 1.37–1.33 (m, 4H), 1.29 (s, 36H), 1.24 (t, ^3J = 7 Hz, 3H), 0.88 ppm (t, ^3J = 7 Hz, 3H); IR (KBr): $\tilde{\nu}$ = 2972, 2867, 1702, 1652, 1590, 1509, 1289 cm^{-1}; MS (MALDI-TOF, pos. mode, dithranol): *m*/*z*: calcd for: 1252.60; found: 1251.79 $[M]^{+\bullet}$; elemental analysis calcd (%) for $C_{79}H_{84}N_2O_{12}$ (1253.52): C 75.69, H 6.75, N 2.23; found: C 75.25, H 6.65, N 2.13.

Acknowledgements

This work was supported by the French National Research Agency (ANR Nanorgysol) and the Conseil Général du Maine et Loire for the grant to J.B. We thank Dr. Jacques Delaunay (CIMA, Université d'Angers) for spectroscopic analyses and Dr Dario Bassani (LCOO, Université Bordeaux 1) for fruitful discussions. BASF-AG (Ludwigshafen) is also acknowledged for providing 1,6,7,12-tetrachloroperylene tetracarboxylic dianhydride. We are grateful to NOW (de Nederlandse Organisatie voor Wetenschappelijk Onderzoek) for the grant for the femtosecond equipment and to the UvA (Universiteit van Amsterdam) for structural support. We thank the Vietnamese Oversea Scholarship Program (VOSP) of the Vietnamese government for the support of N.V.A. within the UvA-HUT project.

[1] R. Huber, *Angew. Chem.* **1989**, *101*, 849–871; *Angew. Chem. Int. Ed. Engl.* **1989**, *28*, 848–869.

[2] D. Gust, T. A. Moore, A. L. Moore, *Acc. Chem. Res.* **2001**, *34*, 40–48.

[3] a) T. J. Meyer, *Acc. Chem. Res.* **1989**, *22*, 163–170; b) M. R. Wasielewski, *Chem. Rev.* **1992**, *92*, 435–461; c) D. Gust, T. A. Moore, A. L. Moore, *Acc. Chem. Res.* **1993**, *26*, 198–205.

[4] For the small reorganization energy, see: a) H. Imahori, K. Hagiwara, T. Akiyama, M. Aoki, S. Taniguchi, T. Okada, M. Shirakawa, Y. Sakata, *Chem. Phys. Lett.* **1996**, *263*, 545–550; b) H. Imahori, N. V. Tkachenko, V. Vehmanen, K. Tamaki, H. Lemmetyinen, Y. Sakata, S. Fukuzumi, *J. Phys. Chem. A* **2001**, *105*, 1750–1756; c) H. Imahori, H. Yamada, D. M. Guldi, Y. Endo, A. Shimomura, S. Kundu, K. Yamada, T. Okada, Y. Sakata, S. Fukuzumi, *Angew. Chem.* **2002**, *114*, 2450–2453; *Angew. Chem. Int. Ed.* **2002**, *41*, 2344–2347; d) S. Fukuzumi, K. Ohkubo, H. Imahori, D. M. Guldi, *Chem. Eur. J.* **2003**, *9*, 1585–1593; e) The internal reorganization energy was first estimated in 1995 to be 0.3 eV (see ref. [55b]).

[5] a) *Fullerenes: Principles and Applications* (Eds.: F. Langa, J.-F. Nierengarten), RSC, Cambridge, **2007**; b) *Fullerene Chemistry, Thematic Issue C. R. Chimie* (Eds.: J.-F. Nierengarten, N. Martín, P. Fowler), **2006**, *9*, 859–1116.

[6] a) H. Imahori, Y. Sakata, *Adv. Mater.* **1997**, *9*, 537–546; b) H. Imahori, *Org. Biomol. Chem.* **2004**, *2*, 1425–1433; c) D. I. Schuster, P. Cheng, S. R. Wilson, V. Prokhorenko, M. Katterle, A. R. Holzwarth, S. E. Braslavsky, G. Klihm, R. M. Williams, C. Luo, *J. Am. Chem.*

Soc. **1999**, *121*, 11599–11600; d) D. I. Schuster, P. Cheng, P. D. Jarowski, D. M. Guldi, C. Luo, L. Echegoyen, S. Pyo, A. R. Holzwarth, S. E. Braslavsky, R. M. Williams, G. Klihm, *J. Am. Chem. Soc.* **2004**, *126*, 7257–7270.

[7] a) M.-S. Choi, T. Yamazaki, I. Yamazaki, T. Aida, *Angew. Chem.* **2004**, *116*, 152–160; *Angew. Chem. Int. Ed.* **2004**, *43*, 150–158; b) H. Imahori, *J. Phys. Chem. B* **2004**, *108*, 6130–6143; c) D. I. Schuster, K. Li, D. M. Guldi, *C. R. Chim.* **2006**, *9*, 892–908.

[8] J. J. M. Halls, R. H. Friend in *Clean Electricity form Photovoltaics* (Eds.: M. D. Archer, R. Hill), Imperial College Press, London, **2001**, 377–445.

[9] P. Hudhomme, J. Cousseau in *Fullerenes: Principles and Applications* (Eds.: F. Langa, J.-F. Nierengarten), RSC, Cambridge, **2007**, 221–265.

[10] a) N. Martín, L. Sánchez, B. Illescas, I. Pérez, *Chem. Rev.* **1998**, *98*, 2527–2547; b) J.-F. Nierengarten, *Sol. Energy Mater. Sol. Cells* **2004**, *83*, 187–199; c) J. L. Segura, N. Martín, D. M. Guldi, *Chem. Soc. Rev.* **2005**, *34*, 31–47; d) P. Hudhomme, *C. R. Chim.* **2006**, *9*, 881–891.

[11] R. A. Marcus, *Pure Appl. Chem.* **1997**, *69*, 13–29.

[12] a) J.-F. Nierengarten, J.-F. Eckert, J.-F. Nicoud, L. Ouali, V. Krasnikov, G. Hadziioannou, *Chem. Commun.* **1999**, 617–618; b) P. A. van Hal, S. C. J. Meskers, R. A. J. Janssen, *Appl. Phys. A* **2004**, *79*, 41–46; c) N. Armaroli, G. Accorsi, J. N. Clifford, J.-F. Eckert, J.-F. Nierengarten, *Chem. Asian J.* **2006**, *1*, 564–574.

[13] P. A. van Hal, E. H. A. Beckers, S. C. J. Meskers, R. A. J. Janssen, B. Jousselme, P. Blanchard, J. Roncali, *Chem. Eur. J.* **2002**, *8*, 5415–5429.

[14] a) J. L. Segura, R. Gómez, N. Martín, C. Luo, D. M. Guldi, *Chem. Commun.* **2000**, 701–702; b) I. B. Martini, B. Ma, T. Da Ros, R. Helgeson, F. Wudl, B. J. Schwartz, *Chem. Phys. Lett.* **2000**, *327*, 253–262.

[15] a) J.-F. Eckert, J.-F. Nicoud, J.-F. Nierengarten, S.-G. Liu, L. Echegoyen, F. Barigelletti, N. Armaroli, L. Ouali, V. Krasnikov, G. Hadziioannou, *J. Am. Chem. Soc.* **2000**, *122*, 7467–7479; b) F. Langa, M. J. Gomez-Escalonilla, J.-M. Rueff, T. M. Figueira Duarte, J.-F. Nierengarten, V. Palermo, P. Samori, Y. Rio, G. Accorsi, N. Armaroli, *Chem. Eur. J.* **2005**, *11*, 4405–4415.

[16] N. S. Sariciftci, L. Smilowitz, A. J. Heeger, F. Wudl, *Science* **1992**, *258*, 1474–1476.

[17] G. Yu, J. Gao, J. C. Hummelen, F. Wudl, A. J. Heeger, *Science* **1995**, *270*, 1789–1791.

[18] a) S. Günes, H. Neugebauer, N. S. Sariciftci, *Chem. Rev.* **2007**, *107*, 1324–1338; b) B. C. Thompson, J. M. J. Fréchet, *Angew. Chem.* **2007**, *120*, 62–82; *Angew. Chem. Int. Ed.* **2007**, *47*, 58–77.

[19] a) [60]PCBM = 1-(3-methoxycarbonyl)propyl-1-phenyl-[6,6]methanofullerene or [6,6]-phenyl C_{61}-butyric acid methyl ester; J. C. Hummelen, B. W. Knight, F. LePeq, F. Wudl, *J. Org. Chem.* **1995**, *60*, 532–538.

[20] C. Winder, N. S. Sariciftci, *J. Mater. Chem.* **2004**, *14*, 1077–1086.

[21] A. Adronov, J. M. J. Frechet, *Chem. Commun.* **2000**, 1701–1710.

[22] G. Accorsi, N. Armaroli, J.-F. Eckert, J.-F. Nierengarten, *Tetrahedron Lett.* **2002**, *43*, 65–68.

[23] M. M. Wienk, J. M. Kroon, W. J. H. Verhees, J. Knol, J. C. Hummelen, P. A. van Hal, R. A. J. Janssen, *Angew. Chem.* **2003**, *115*, 3493–3497; *Angew. Chem. Int. Ed.* **2003**, *42*, 3371–3375.

[24] F. Würthner, *Chem. Commun.* **2004**, 1564–1579.

[25] H. Langhals, S. Saulich, *Chem. Eur. J.* **2002**, *8*, 5630–5643.

[26] a) X. Guo, D. Zhang, H. Zhang, Q. Fan, W. Xu, X. Ai, L. Fan, D. Zhu, *Tetrahedron* **2003**, *59*, 4843–4850; b) S. Leroy-Lhez, J. Baffreau, L. Perrin, E. Levillain, M. Allain, M.-J. Blesa, P. Hudhomme, *J. Org. Chem.* **2005**, *70*, 6313–6320.

[27] B. K. Kaletas, R. Dobrowa, A. Sautter, F. Würthner, M. Zimine, L. De Cola, R. M. Williams, *J. Phys. Chem. A* **2004**, *108*, 1900–2909.

[28] a) C.-C. You, C. R. Saha-Möller, F. Würthner, *Chem. Commun.* **2004**, 2345–2348; b) L. X. Chen, S. Xiao, L. Yu, *J. Phys. Chem. A* **2006**, *110*, 11730–11738.

[29] X. Li, L. E. Sinks, B. Rybtchinski, M. R. Wasielewski, *J. Am. Chem. Soc.* **2004**, *126*, 10810–10811.

[30] J. L. Segura, R. Gómez, E. Reinold, P. Bäuerle, *Org. Lett.* **2005**, *7*, 2345–2348.

[31] R. F. Kelley, M. J. Tauber, M. R. Wasielewski, *J. Am. Chem. Soc.* **2006**, *128*, 4779–4791.

[32] T. Ishi-i, K. Murakami, Y. Imai, S. Mataka, *J. Org. Chem.* **2006**, *71*, 5752–5760.

[33] M. Takahashi, H. Morimoto, K. Miyake, M. Yamashita, H. Kawai, Y. Sei, K. Yamaguchi, *Chem. Commun.* **2006**, 3084–3086.

[34] S. Leroy-Lhez, L. Perrin, J. Baffreau, P. Hudhomme, *C. R. Chim.* **2006**, *9*, 240–246.

[35] M. D. Yilmaz, O. A. Bozdemir, E. U. Akkaya, *Org. Lett.* **2006**, *8*, 2871–2873.

[36] R. Gómez, D. Veldman, R. Blanco, C. Seoane, J. L. Segura, R. A. J. Janssen, *Macromolecules* **2007**, *40*, 2760–2772.

[37] E. E. Neuteboom, E. H. A. Beckers, S. C. J. Meskers, E. W. Meijer, R. A. J. Janssen, *Org. Biomol. Chem.* **2003**, *1*, 198–203.

[38] M. S. Rodriguez-Morgade, T. Torres, C. Atienza-Castellanos, D. M. Guldi, *J. Am. Chem. Soc.* **2006**, *128*, 15145–15154.

[39] H. Li, Y. Wang, W. Zhang, B. Liu, G. Calzaferri, *Chem. Commun.* **2007**, 2853–2854.

[40] J. Baffreau, L. Perrin, S. Leroy-Lhez, P. Hudhomme, *Tetrahedron Lett.* **2005**, *46*, 4599–4603.

[41] a) J. L. Hua, F. S. Meng, F. Ding, H. Tian, *Chem. Lett.* **2004**, *33*, 432–433; b) J. L. Hua, F. S. Meng, F. Ding, F. Y. Li, H. Tian, *J. Mater. Chem.* **2004**, *14*, 1849–1853; c) Y. Liu, N. Wang, Y. J. Li, H. B. Liu, J. H. Xiao, X. H. Xu, C. S. Huang, S. Cui, D. B. Zhu, *Macromolecules* **2005**, *38*, 4880–4887; d) R. Gómez, J. L. Segura, N. Martín, *Org. Lett.* **2005**, *7*, 717–720; e) Y. Li, Y, Li, H. Liu, S. Wang, N. Wang, J. Zhuang, X. Li, X. He, D. Zhu, *Nanotechnology* **2005**, *16*, 1899–1904; f) N. Wang, Y. J. Li, X. R. He, H. Y. Gan, Y. L. Li, C. S. Huang, X. H. Xu, J. C. Xiao, S. Wang, H. B. Liu, D. B. Zhu, *Tetrahedron* **2006**, *62*, 1216–1222; g) Y. Shibano, T. Umeyama, Y. Matano, N. V. Tkachenko, H. Lemmetyinen, H. Imahori, *Org. Lett.* **2006**, *8*, 4425–4428; h) Y. Shibano, T. Umeyama, Y. Matano, N. V. Tkachenko, H. Lemmetyinen, Y. Araki, O. Ito, H. Imahori, *J. Phys. Chem. C* **2007**, *111*, 6133–6142.

[42] a) Y. Nagao, T. Misono, *Bull. Chem. Soc. Jpn.* **1981**, *54*, 1191–1194; b) H. Tröster, *Dyes Pigm.* **1983**, *4*, 171- 177; c) H. Kaiser, J. Lindner, H. Langhals, *Chem. Ber.* **1991**, *124*, 529–535.

[43] a) G. Seybold, A. Stange, BASF AG Patent, DE 3545004, **1987**; b) G. Seybold, G. Wagenblast, *Dyes Pigm.* **1989**, *11*, 303–317.

[44] F. Würthner, C. Thalaker, A. Sautter, W. Schärtl, W. Ibach, O. Hollricher, *Chem. Eur. J.* **2000**, *6*, 3871–3886.

[45] a) J.-F. Nierengarten, V. Gramlich, F. Cardullo, F. Diederich, *Angew. Chem.* **1996**, *108*, 2242–2244; *Angew. Chem. Int. Ed. Engl.* **1996**, *35*, 2101–2103; b) J.-F. Nierengarten, A. Herrmann, R. R. Tykwinski, M. Ruttimann, F. Diederich, *Helv. Chim. Acta* **1997**, *80*, 293–316; c) R. Kessinger, J. Crassous, A. Herrmann, M. Ruttimann, L. Echegoyen, F. Diederich, *Angew. Chem.* **1998**, *110*, 2022–2025; *Angew. Chem. Int. Ed.* **1998**, *37*, 1919–1922.

[46] a) M. Karplus, *J. Chem. Phys.* **1959**, *30*, 11–15; b) M. Karplus, *J. Am. Chem. Soc.* **1963**, *85*, 2870–2871.

[47] H. Friebolin, *Basic One- and Two-Dimensional NMR Spectroscopy*, VCH, Weinheim, **1991**, 73–94.

[48] J. Baffreau, S. Leroy-Lhez, N. Gallego-Planas, P. Hudhomme, *J. Mol. Struct.* **2007**, *815*, 145–150.

[49] H. Günther, *NMR Spectroscopy*, Wiley, New York, **1980**, 234–280.

[50] C. Bingel, *Chem. Ber.* **1993**, *126*, 1957–1959.

[51] H. Langhals, S. Demmig, H. Huber, *Spectrochim. Acta Part A* **1988**, *44*, 1189–1193.

[52] S. Prathapan, S. I. Yang, J. Seth, M. A. Miller, D. F. Bocian, D. Holten, J. S. Lindsey, *J. Phys. Chem. B* **2001**, *105*, 8237–8248.

[53] W. E. Ford, P. V. Kamat, *J. Phys. Chem.* **1987**, *91*, 6373–6380.

[54] C. Addicott, I. Oesterling, T. Yamamoto, K. Müllen, P. J. Stang, *J. Org. Chem.* **2005**, *70*, 797–801.

[55] a) S. M. Anthony, S. M. Bachilo, R. B. Weisman, *J. Phys. Chem. A* **2003**, *107*, 10674–10679; b) R. M. Williams, J. M. Zwier, J. W. Verhoeven, *J. Am. Chem. Soc.* **1995**, *117*, 4093–4099; c) R. M. Williams,

M. Koeberg, J. M. Lawson, Y.-Z. An, Y. Rubin, M. N. Paddon-Row, J. W. Verhoeven, *J. Org. Chem.* **1996**, *61*, 5055–5062.
[56] D. M. Guldi, K.-D. Asmus, *Proc. SPIE-Int. Soc. Opt. Eng.* **1996**, *2854*, 236–245.
[57] B. Ma, C. E. Bunker, R. Guduru, X.-F. Zhang, Y.-P. Sun, *J. Phys. Chem. A* **1997**, *101*, 5626–5632.
[58] a) T. Z. Förster, *Naturforsch. A* **1949**, *4*, 321–327; b) T. Z. Förster, *Discuss. Faraday Soc.* **1959**, *27*, 7–17.
[59] D. L. Dexter, *J. Chem. Phys.* **1953**, *21*, 836–850.
[60] D. Rehm, A. Weller, *Isr. J. Chem.* **1970**, *8*, 259–271.
[61] We attribute this to the presence of a PDI derivative impurity in spite of repetitive efforts to purify dyads by preparative HPLC. Indeed, taking into account both the relative emission intensity and amplitudes of the long-lived components, the amounts could be estimated to be 0.003 to 0.015%, implying 99.997 and 99.985% purity (!) of the dyads. A second hypothesis considers that this long-lived component could be also due to a non-active conformation of the dyad.
[62] R. Gvishi, R. Reisfeld, Z. Burshtein, *Chem. Phys. Lett.* **1987**, *213*, 338–344.
[63] a) M. E. El-Khouly, P. Padmawar, Y. Araki, S. Verma, L. Y. Chiang, O. Ito, *J. Phys. Chem. A* **2006**, *110*, 884–891; b) T. Nakamura, H. Kanato, Y. Araki, O. Ito, K. Takimiya, T. Otsubo, Y. Aso, *J. Phys. Chem. A* **2006**, *110*, 3471–3479.
[64] A. Sautter, B. K. Kaletas, D. G. Schmid, R. Dobrawa, M. Zimine, G. Jung, I. H. M. van Stokkum, L. De Cola, R. M. Williams, F. Würthner, *J. Am. Chem. Soc.* **2005**, *127*, 6719–6729.
[65] J. Baffreau, S. Leroy-Lhez, P. Hudhomme, M. M. Groeneveld, I. H. M. van Stokkum, R. M. Williams, *J. Phys. Chem. A* **2006**, *110*, 13123–13125.
[66] T. W. Ebbesen, K. Tanigaki, S. Kuroshima, *Chem. Phys. Lett.* **1991**, *181*, 501–504.
[67] W. E. Ford, H. Hiratsuka, P. V. Kamat, *J. Phys. Chem.* **1989**, *93*, 6692–6696.
[68] S. D. Yao, Z. R. Lian, W. F. Wang, J. S. Zhang, N. Y. Lin, H. Q. Hou, Z. M. Zhang, Q. Z. Qin, *Chem. Phys. Lett.* **1995**, *239*, 112–116.
[69] T. Kato, T. Kodama, M. Oyama, S. Okazaki, T. Shida, T. Nakagawa, Y. Matsui, S. Suzuki, H. Shiromaru, K. Yamauchi, Y. Achiba, *Chem. Phys. Lett.* **1991**, *186*, 35–39.
[70] A. Prodi, C. Chiorboli, F. Scandola, E. Iengo, E. Alessio, R. Dobrawa, F. Würthner, *J. Am. Chem. Soc.* **2005**, *127*, 1454–1462.
[71] T. van der Boom, R. T. Hayes, Y. Zhao, P. J. Bushard, E. A. Weiss, M. R. Wasielewski, *J. Am. Chem. Soc.* **2002**, *124*, 9582–9590.
[72] R. V. Bensasson, E. Bienvenüe, C. Fabre, J.-M. Janot, E. J. Land, S. Leach, V. Leboulaire, A. Rassat, S. Roux, P. Seta, *Chem. Eur. J.* **1998**, *4*, 270–278.
[73] R. Bonneau, I. Carmichael, G. L. Hug, *Pure Appl. Chem.* **1991**, *63*, 289–299.
[74] J. Li, N. Sun, Z.-X. Guo, C. Li, Y. Li, L. Dai, D. Zhu, *J. Phys. Chem. B* **2002**, *106*, 11509–11514.
[75] a) C. Hippius, F. Schlosser, M. O. Vysotsky, V. Böhmer, F. Würthner, *J. Am. Chem. Soc.* **2006**, *128*, 3870–3871; b) C. Hippius, I. H. M. van Stokkum, M. Gsänger, M. M. Groeneveld, R. M. Williams, F. Würthner, *J. Phys. Chem. A* **2008**, *112*, 2476–2486.
[76] J. Baffreau, S. Leroy-Lhez, H. Derbal, A. R. Inigo, J.-M. Nunzi, M. M. Groeneveld, R. M. Williams, P. Hudhomme, *Eur. Phys. J. Appl. Phys.* **2006**, *36*, 301–305.

Received: January 25, 2008
Published online: April 16, 2008

